DOI: 10.26599/FSHW.2025.9250824

Contents lists available at SciOpen

Food Science and Human Wellness

journal homepage: https://www.sciopen.com/journal/2097-0765

China Food Publishing Co.

Nicotinamide mononucleotide (NMN) improves ovarian inflammation via lactate-mediated NLRP3 modifications in premature ovarian insufficiency

Siyuan Lei [1#], Haoxuan Xue [1#], Ke Liu [1#], Yue Ma [1], Yanhong Wei [2], Linlin Hu [2], Qiumei Huang [2], Jiameng Yang [1], Wenhui Zou[1], Kongwei Huang [1], Xiaocan Lei [1*]

[1.] *Clinical Anatomy and Reproductive Medicine Application Institute, The First Affiliated Hospital, Hengyang Medical School, University of South China, Hengyang 421001, China.*

[2.] *Key Laboratory of Research on Clinical Molecular Diagnosis for High Incidence Diseases in Western Guangxi, Department of Obstetrics and Gynecology, Affiliated Hospital of Youjiang Medical University for Nationalities, Baise, Guangxi 533000, China.*

ABSTRACT: Premature ovarian insufficiency (POI) significantly impacts female fertility, yet its mechanisms and treatment strategies remain unclear. This study aimed to elucidate POI pathogenesis and identify potential therapies. NMN is an orally bioavailable NAD+ precursor naturally present in various foods, was investigated as a therapeutic agent. A rat model of POI revealed upregulation of inflammatory cytokines, including NLRP3, IL-1β, and IL-18. Treatment with NMN and estradiol (E2) improved ovarian reserve function, with NMN notably increasing lactate production in ovaries and granulosa cells (GCs). Western blotting showed altered protein acetylation and lactylation levels in the rat ovarian tissues, modulated by lactate, which was found to bind to lysine residues on NLRP3. Adding sodium lactate decreased NLRP3 acetylation while increasing lactylation. All seven mammalian SIRT isoforms (SIRT1–7) were initially screened, revealing that SIRT3 inhibits NLRP3 acetylation, SIRT2 is a main de-lactylase, and PCAF is a common writer for NLRP3 acetylation and lactylation. Additionally, the acetylation and lactylation modification sites of the NLRP3 protein were identified as K570 and K599, respectively. Lastly, lactate inhibited NLRP3 and downstream inflammatory cytokines in the human granulosa-like tumor cell line KGN. These findings suggest that lactate regulates NLRP3 modifications, providing new therapeutic targets for POI treatment.

Keywords: Premature ovarian insufficiency; NLRP3; Lactylation; Acetylation; Lactate

1. Introduction

Premature ovarian insufficiency (POI) has emerged as a significant global health issue related to infertility, defined as premature ovarian reserve decline in women under 40, characterized primarily by menstrual irregularities, elevated levels of gonadotropins (FSH > 25 U/L), and fluctuating estrogen.[1] Currently, the global incidence of POI is approximately 3.7%, influenced by genetic, autoimmune, iatrogenic, environmental, and lifestyle factors, with increasing incidence and a trend towards younger ages.[2] The pathogenesis of POI remains unclear, posing substantial risks to female reproductive function.[3, 4] There is an urgent need to explore effective treatment methods.

# Authors contributed equally to this work.
***Corresponding author**
2019000013@usc.edu.cn.

Received 28 April 2025
Received in revised from 25 June 2025
Accepted 25 July 2025

POI is increasingly linked to NLRP3 inflammasome-driven inflammatory aging.[5] NLRP3, known for its pivotal role in various inflammatory and age-related disorders, promotes caspase-1-dependent IL-1β, IL-18 and the cleavage of GSDMD.[6] Clinical studies show that the expression levels of inflammatory factors such as NLRP3, IL-1β and IL-18 are elevated in the oocytes and granulosa cells of patients with POI.[7] Reducing these markers alleviates endocrine dysfunction and ovarian reserve.[5, 8] Therefore, the role of NLRP3-mediated inflammation in the decline of ovarian function, have become key research topics in the current study of POI. On the other hand, lactate is a key energy source for oocyte maturation and follicular development.[9] Glycolytic inhibition reduces lactate levels, leading to increased NLRP3, TNF-α, and IL-6， lactate supplementation suppresses NLRP3 inflammasome formation and IL-1β secretion.[10] Exploring the relationship between lactate and NLRP3-mediated inflammatory senescence may provide new approaches to enhance ovarian reserve function in patients with POI.

NMN, a compound widely utilized as a dietary supplement and cosmetic ingredient, serves as a critical NAD+ precursor that rapidly converts to NAD+ to modulate oxidative stress, DNA repair, and inflammatory responses.[11, 12] Notably, NMN-mediated NAD+ elevation concomitantly enhances lactate production in mammalian cells.[13] Recent studies reveal lactate's dual role as both a metabolic intermediate and a signaling molecule,[14] which can modulate protein acetylation to influence NLRP3 inflammasome activation.[15-17] Additionally, lactate donates lactyl groups to substrate proteins via lactyl-CoA, leading to lactylation modifications that regulate the function of target genes.[18-20] Notably, lactate demonstrates significant organ-protective properties, including cardioprotective and neuroprotective effects through its anti-inflammatory actions,[21] while also suppressing NLRP3 inflammasome activation in macrophages via specific histone modifications (H3K9 acetylation and H3K18 lactylation).[22] These findings collectively underscore lactate's pivotal role at the intersection of cellular metabolism and inflammatory regulation.

This study aims to elucidate the role of lactate in regulating NLRP3 to improve ovarian reserve decline in POI. It involves screening and identifying key modifying enzymes and functional sites that regulate NLRP3 acetylation/lactylation, thereby uncovering and validating the molecular mechanisms through which lactate enhances POI ovarian reserve function. It provides new strategies and targets for the diagnosis and treatment of ovarian reserve decline in clinical POI patients.

2. Materials and methods

2.1 Animals and Treatment

A total of 40 female Sprague Dawley rats (8 weeks old, 200 g ± 50 g) were procured from the Changsha Tianqing Company. All rats were kept in standard environmental conditions (25℃, 12 h light/dark cycle) with free access to standard food pellets and water, until the experiments started. The body weights of the animals were recorded periodically. After one week of adaptive feeding, all rats were randomly divided into 4 different groups: the control group (Control, n=10), the POI model group (POI, n=10), the E2 treatment group (POI-E2, n=10) and the NMN treatment group (POI-NMN, n=10). The Control group and POI group were administered with 0.9% saline by intragastric administration, while the POI-E2 group was intragastric administration with

E2 (0.1 mg/kg/day) and the POI-NMN group was intragastric administration with NMN (500 mg/kg/day)[23] for 42 days until the end of the experiment. After intragastric administration seven days, the rats of POI group, POI-E2 group and POI-NMN group were intraperitoneally injected with CTX (50 mg/kg/day on the first day, the dose for the following 13 days is 8 mg/kg) for 14 days[24], while the rats in Control group were injected with an equivalent volume of 0.9% saline. Vaginal smears were taken 10 days before the end of modeling to observe the changes of estrous cycle in SD rats, preliminarily judge whether this model was successful. At the end of the experiment all rats were anesthetized with 20% urethane. With the animals under deep anesthesia, a 3 cm incision was made along the midline of the abdomen to separate the subcutaneous connective tissue and abdominal muscles. Immediately, whole blood samples were collected from the abdominal aorta of the rats, followed by the ovariectomy procedure to remove the left and right ovaries. Subsequently, the blood was centrifuged at 3,000 r/min for 10 minutes to separate the serum. All animal procedures and experiments are approved by the Animal Ethics Committee of University of South China (USC2020031602).

2.2 Estrous Cycle Analysis

Consecutive vaginal smears were conducted for 10 days at 12:00 before the completion of the modeling process. In brief, 10 μL of 0.9% NaCl was used to rinse the vagina two or three times, and the collected vaginal fluid was smeared onto a slide. Following air drying, the vaginal smears were stained with Liu stain (Baso, Zhuhai, China) as per the manufacturer's protocol. Observations of the changes in vaginal epithelial cells were made under a light microscope to assess the stages estrous cycle (proestrus, estrus, diestrus, and diestrus) .

2.3 Morphological Analysis of The Ovary and Follicular Classification

The ovaries from each rat were fixed in 4% formaldehyde (BL539A, biosharp Co.) for 24 h, followed by embedding in paraffin and slicing into 5 μm-thick sections (HI1210, Leica, Germany). Following this, the sections underwent staining with hematoxylin and eosin (H&E). Observation of ovarian morphological characteristics under a microscope. To quantify the number of follicles in each ovary, we stained and analyzed five consecutive sections. Following the method outlined by Pedersen and Peters, follicles at different stages were counted in a double-blind manner, and the final count was multiplied by five.

2.4 Measurement of Hormone Concentrations

After all rats were anesthetized with 20% urethane, whole blood was collected via abdominal aortic puncture and centrifuged at 4℃ (3,000×g) (5804R, Eppendorf, Germany) for 15 minutes to separate serum. Finally, the levels of follicle-stimulating hormone (FSH) and estrogen (E2) in rat serum were determined using radioimmunoassay, while the concentration of anti-Müllerian hormone (AMH) was measured using enzyme-linked immunosorbent assay (ELISA).(Ruixinbio, Quanzhou, China)

2.5 Masson Assay

The ovarian sections embedded in paraffin were subjected to routine deparaffinization and hydration processes. They were stained with hematoxylin for 10 min, followed by a 10-second immersion in acid

alcohol and a 2-min rinse in running water. Subsequently, they were stained with Masson's blue solution for 5 min, rinsed in running water for 2 min, and then stained with Acid Fuchsin solution for 5 min. After a 5-second wash in 2% acetic acid, the sections were immersed in 1% phosphomolybdic acid solution for 5 min, followed by staining with Aniline Blue solution for 5 min. A 1-min immersion in acetic acid was followed by dehydration in 95% ethanol and absolute ethanol, clearing in xylene, mounting with neutral resin, and examination under the microscope.

2.6 Immunohistochemical Assay

For the immunohistochemistry (IHC) study of ovarian tissue samples, the samples were fixed overnight in 4% paraformaldehyde, embedded in paraffin, and cut into 5μm consecutive sections. Endogenous peroxidase activity was blocked in 3% H2O2 for 30 minutes. The sections underwent antigen retrieval three times in a 0.1M pH 6.0 sodium citrate buffer using a microwave, followed by permeabilization in 1% Triton X-100 and PBST for 30 minutes, and blocking with 5% bovine serum albumin for 45 minutes. Then these sections were incubated with primary antibodies including rabbit LDHA (1:200 dilution, T58276, Abmart Shanghai Co.,Ltd.) , NLRP3 (1:200 dilution, T55651, Abmart Shanghai Co.,Ltd.), IL-1β (1:200 dilution, T55651, Abmart Shanghai Co.,Ltd.) and IL-18 (1:200 dilution, TD6252, Abmart Shanghai Co.,Ltd.) overnight at 4℃. Following PBS-T washing, the sections underwent a 90-min incubation at room temperature with the Biotin-SP-conjugated Affinipure Rabbit Anti-Goat IgG(H+L) (1:200, SA00004–4; Protein Tech Group Inc.), followed by a 45-min incubation with HRP-conjugated Streptavidin (1:200, SA00001–0; Protein Tech Group Inc.). After another round of washing with PBS-T, the immunoreactivity of the target proteins was visualized utilizing DAB (20×Metal Enhanced DAB Substrate Kit; Solarbio), followed by counter-staining with hematoxylin. PBST was used as a negative control. The stained sections were ultimately inspected and captured through a light microscope (BX43, Olympus, Tokyo, Japan).

2.7 Cell Culture and Treatment

All cell lines (KGN,293T) used in this study were obtained from the Institute of Clinical Anatomy & Reproductive Medicine. Cells were cultured in Dulbecco's Modified Eagle Medium (DMEM, Sigma, USA) with 10% fetal bovine serum (FBSST-01033-500, Oricell, Guangzhou, China) at 37℃ with 5% CO2. Subsequent experiments were carried out using KGN cells, which underwent the following interventions: (1)Cells were either left untreated or treated with CTX (4 μg/ml, C0768, Sigma, USA), LPS (1μg/ml, L4391, Sigma, USA)+Nig (10 μmol/L, HY-100381, MedChemExpress, USA),[25] or CTX+NMN (50 μmol/L, N3501, Sigma, USA).[23] (2)Cells were either left untreated or treated with Cocl2 (100 μmol/L,C8661, Sigma, USA),[26] Cocl2+2-DG (1mmol/L, D8375, Sigma, USA), or Cocl2+LPS+Nig. (3)Cells were either left untreated or treated with Lactate (10 mmol/L, L6402, Sigma, USA), 2-DG, or 2-DG+NMN. After treatment for 24 hours, the proteins and the RNA were collected for western blot analysis and qRT-PCR. The supernatant was collected for lactate level detection and anti-Müllerian hormone (AMH) detection, while cells were collected for NAD^+ level detection. 293T cells underwent the following interventions: (1) Cells transfected with Flag-NLRP3 as a control, combined with sodium lactate (NaLa, 20 mmol/L) or Oxamate (20

mmol/L, an inhibitor of LDHA, O2751, Sigma, USA).[27, 28] (2) Cells transfected with Flag-NLRP3 as a control or co-transfect with LDHA shRNA. (3) Cells transfected with Flag-NLRP3 as a control, combined with a broad-spectrum HDAC inhibitor (trichostatin A, TSA, 500 nmol/L, T1952, Sigma, USA) or a sirtuin inhibitor (nicotinamide, NAM, 10 mmol/L, BP460, Sigma, USA).[27] (4) Cells transfected with Flag-NLRP3 as a control or co-transfect with overexpression plasmids for SIRT1-7, PCAF, GCN5, P300, and CBP. (5) Transfect with plasmids containing mutations at acetylation and lactylation sites.

2.8 Cell viability assay

A CCK-8 assay kit (BS350B, biosharp, China) determined the cell viability in 96-well plates according to the manufacturer's instructions. Each well of a 96-well plate should have a KGN cell density of 5×10^3 cells. The KGN cells was treated with CTX at concentrations of 0, 2, 4 and 8 μg/ml and normal saline for 24 h[29], respectively. Then 10 μL CCK-8 reagent was added to each well and then continuously incubated for 1–3 h at 37 ℃ in darkness. Finally, a PerkinElmer microplate reader was used to determine the absorbance.

2.9 Cell Transfection

Two hours prior to transfection, replace the culture medium with serum-free medium. For the transfection, use 2-4 μg of plasmid DNA and 10-20 μL of Lipofectamine 5000 (21024, BIOG, Changzhou, China). Dilute the plasmid DNA in Opti-MEM (31985070, Gibco, USA), then mix it with the transfection reagent and incubate at room temperature for 20 minutes. After incubation, evenly add the Lipofectamine 5000-DNA complex to the culture dish. Incubate for 18 hours, then replace the medium with serum-containing medium. Following this treatment, collect proteins for experiments.

2.10 Western Blotting

For western blotting, ovarian tissues and KGN cells were added into lysate (containing 1% PMSF) and fully lysed on ice for 30 minutes. The supernatant was collected by centrifugation(4℃, 12000 r/min, 20 min). Protein concentrations were measured with a BCA Protein Assay Kit (CW0014S, Beijing ComWin Biotech Co., Ltd. Beijing, China) and the protein was denatured by boiling at 100℃ for 10 min in sample buffer. A total of 40 μg protein tissues or cell lysates were separated by 10% SDS-PAGE (CW0022S, Beijing ComWin Biotech Co., Ltd. Beijing, China) and transferred to PVDF membranes (Millipore, Billerica, MA, USA), which were then blocked with 5% skim milk for 2h at room temperature. The blots were incubated with the primary rabbit monoclonal antibodies including HK2 (1:1000 dilution, TD6176, Abmart Shanghai Co.,Ltd.), PKM2 (1:1000 dilution, T55764, Abmart Shanghai Co.,Ltd.), LDHA (1:1000 dilution, T58276, Abmart Shanghai Co.,Ltd.), NLRP3 (1:1000 dilution, T55651, Abmart Shanghai Co.,Ltd.), CASPASE-1 (1:1000 dilution, TD6252, Abmart Shanghai Co.,Ltd.), GSDMD (1:1000 dilution, TA4012, Abmart Shanghai Co.,Ltd.), IL-1β (1:1000 dilution, T55651, Abmart Shanghai Co.,Ltd.), IL-18 (1:1000 dilution, TD6252, Abmart Shanghai Co.,Ltd.), DYKDDDDK-Tag(3B9) mAb (1:5000 dilution, M20008, Abmart Shanghai Co.,Ltd.), Anti-HA-Tag Antibody(1:5000 dilution, M20021, Abmart Shanghai Co.,Ltd.), Anti-L-Lactyllysine(1:1000 dilution，PTM-1401, PTM Biolabs) and Anti-Acetyllysine(1:1000 dilution，

PTM-105RM，PTM Biolabs) overnight at 4℃. β-tubulin (1:5000 dilution, R20005, Abmart Shanghai Co.,Ltd.) was used as the loading control. Finally, the blots were exposed to eECL (CW0049M, Beijing ComWin Biotech Co, Ltd. Beijing, China) and a Tanon-5500 Chemiluminescence Imaging System (Tanon5500, Tanon, Shanghai, China.) was used to detect the chemiluminescence of protein bands. Blotting images were using Image J analysis software (JAVA image processing program, NIH, Bethesda, MD, USA).

2.11 Real-Time Quantitative PCR (qRT-PCR) Analysis

Total RNA was extracted from ovaries and KGN cells using Trizol reagent (15596026; Thermo Fisher Scientific, Shanghai, China), then reverse transcribed to cDNA with a TransScript® One-Step135 gDNA Removal (TransGen Biotech, Beijing, China) and cDNA synthesis SuperMix kit (AT311-02, Transgen Biotech, China, Beijing) according to the manufacturer's protocol, qRT-PCR was performed in 10 μL volumes by 2× Universal SYBR Green Fast qPCR Mix kit (A35379, Thermo Fisher Scientific) and Applied Biosystems QuantStudio 3 (A28136, Thermo Fisher Scientific). The comparative CT method was used to calculate gene expression differences, with GAPDH as the reference gene. The primers were designed and synthesized by Shanghai Sangon151 Biotechnology Co., Ltd. Shanghai, China. Primers for the amplification reaction are listed in Table 1.

Table 1 Primer sequences used for the qRT-PCR analysis

Gene ID		Sequence	Accession NO.
RAT NLRP3	Forward	GAGCTGGACCTCAGTGACAATGC	XM 006246457.4
	Reverse	AGAACCAATGCGAGATCCTGACAAC	
RAT Caspase-1	Forward	GACCGAGTGGTTCCCTCAAG	NM 012762.3
	Reverse	GACGTGTACGAGTGGGTGTT	
RAT GSDMD	Forward	ATTGGCTCTGAATGGGATA	NM 001400994.1
	Reverse	CGGCACCAGTTCTCCA	
RAT IL-1β	Forward	CCCTTGTCGAGAATGGGCAG	NM 031512.2
	Reverse	GACCAGAATGTGCCACGGTT	
RAT IL-18	Forward	CGACCGAACAGCCAACGAATCC	NM 019165.2
	Reverse	GTCACAGCCAGTCCTCTTACTTCAC	
RAT GAPDH	Forward	GAGTCCACTGGCGTCTTCAC	XM 032916238
	Reverse	GAGGCATTGCTGATGATCTTGAG	
Homo NLRP3	Forward	ATGCTGCTTCGACATCTCCT	XM 047443562.1
	Reverse	AACCAATGCGAGATCCTGAC	
Homo Caspase-1	Forward	TTTCCGCAAGGTTCGATTTTCA	XM 017018396
	Reverse	GGCATCTGCGCTCTACCATC	
Homo GSDMD	Forward	CAGAAGGGACGTGGTGTTCC	NM 001166237
	Reverse	AAGTGTTGAGGGCAGAACCC	
Homo IL-1β	Forward	CTCGCCAGTGAAATGAT	NM 000576
	Reverse	AAGCCCTTGCTGTAGTG	
Homo IL-18	Forward	ATGGCTGCTGAACCAGTAGAAGAC	NM 001243211.2
	Reverse	TCCGGGGTGCATTATCTCTACAGTC	
Homo GAPDH	Forward	GGATTTGGTCGTATTGGGCG	NM 001357943.2
	Reverse	TCCCGTTCTCAGCCATGTAG	
RAT	Forward	TTGCCTACTTCTTCACGGAG	NM 012735.2

HK2	Reverse	TCTGGAGTGGACCTCACAAAG	
RAT PKM2	Forward	GGAACACTGGCATCATCTGTA	XM 039080895.1
	Reverse	TCGGATCTCAGGTCCTTTAGT	
RAT LDHA	Forward	GGTTGACAGTGCATACGAAG	XM 039082293
	Reverse	CCGCCTAAGGTTCTTCATTA	
Homo HK2	Forward	GTGAACGATGCTCCTGCTCTGAAG	M23115.1
	Reverse	CTCCTCAACGGCAGCCACAATG	
Homo PKM2	Forward	GAGTCCACTGGCGTCTTCAC	KJ905271.1
	Reverse	GAGGCATTGCTGATGATCTTGAG	
Homo LDHA	Forward	ATGAGTTGGACTGTGCCTGTTGTG	AY009108.1
	Reverse	GTGAAGAGCCAGGTGCCGTTG	

2.12 Measurement of Lactate and NAD+ Level

The lactate and NAD^+ levels were measured separately using a lactate assay kit (Cat. #A019-2-1, Nanjing Jiancheng Bioengineering Institute) and a Coenzyme I NAD(H) assay kit (Cat. #A114-1-1, Nanjing Jiancheng Bioengineering Institute), following the manufacturer's instructions.

2.13 Enzyme-Linked Immunosorbent Assay (ELISA)

AMH in the culture supernatant and rat ovarian tissues were measured by commercially available ELISA kits (Ruixinbio, Quanzhou, China). Plates were read on a VersaMax microplate reader at 450 nm wavelengths.

2.14 Co-immunoprecipitation (Co-IP)

Following transfection, 293T cells were lysed in an appropriate volume of protein lysis buffer (supplemented with protease inhibitors) on ice for 30 minutes. The lysates were then centrifuged at 12,000 × g for 15 minutes at 4℃ to collect the supernatant. A small aliquot of the protein lysate was reserved for Western Blotting analysis. The remaining lysate was incubated with anti-Flag magnetic beads (MA101-25T, ABMagic Biotech, Shenzhen, China) for 2 hours at 4℃ with gentle rotation to allow immunoprecipitation. After the immunoprecipitation reaction, the supernatant was carefully removed while retaining the beads. The beads were washed three times with ice-cold washing buffer (1× PBS containing 0.1% Tween-20). After complete removal of the washing buffer, the beads were resuspended in 2× Laemmli loading buffer and boiled at 95℃ for 10 minutes to elute the immunoprecipitated proteins. The eluted proteins were then subjected to SDS-PAGE followed by Western Blotting analysis according to standard protocols.

2.15 Liquid Chromatography-mass Spectrometry (LC-MS)

For acetylation/lactylation site identification, Flag-NLRP3 was overexpressed in cultured 293T cells. The cells were lysed, and the protein extract was incubated with anti-Flag magnetic beads for immunoprecipitation (Co-IP). After incubation, the supernatant was carefully removed, and the beads were washed three times with IP wash buffer. The immunoprecipitated proteins were eluted in 2× Laemmli buffer by boiling at 95℃ for 10 min, followed by SDS-PAGE separation. The target protein band was excised from the gel and sent to Jingjie PTM BioLab (Hangzhou, China) for LC-MS-based acetylation/lactylation site identification.

2.16 Site-directed Mutagenesis

Human NLRP3 plasmid, SIRT1-7 plasmid, PCAF、GCN5、CBP、P300 plasmid, knockdown plasmid and NLRP3 site-mutated plasmid were purchased from VectorBuilder (Guangzhou, China). The mutation was confirmed by DNA sequencing conducted in Shanghai Sangon151 Biotechnology Co., Ltd. (Shanghai, China).

2.17 Statistical Analysis

Data were analyzed using GraphPad Prism 9.0 (GraphPad Software, CA, USA) and presented as the mean ± standard deviation. Significant differences between/within groups were evaluated by the unpaired T-test or one-way ANOVA followed by Bonferroni's post-hoctest. Correlation between variables was determined by Pearson's correlation coefficient. *P* value <0.05 was considered to be statistically significant.

3. Results

3.1 NMN and E2 treatment improved the ovarian reserve function of POI rats

To evaluate the effects of NMN and E2, we developed a CTX-induced rat model of POI, which exhibited ovarian morphology, histological changes, and hormonal alterations resembling those observed in clinical POI patients. After NMN and E2 respectively treatment for 21 days (Figure 1A), the body weight of POI rats did not change significantly during the whole experimental period. The disrupted estrous cycle is an important characteristic of POI rats, whereas the control group rats have an estrous cycle of 4-5 days, consisting of proestrus, estrus, metestrus, and diestrus phases. The rats of POI show an interrupted estrous cycle with prolonged diestrus and shortened proestrus and estrus phases; this abnormal estrous cycle gradually returns to normal after the administration of NMN and E2 (Figure 1B and 1C).

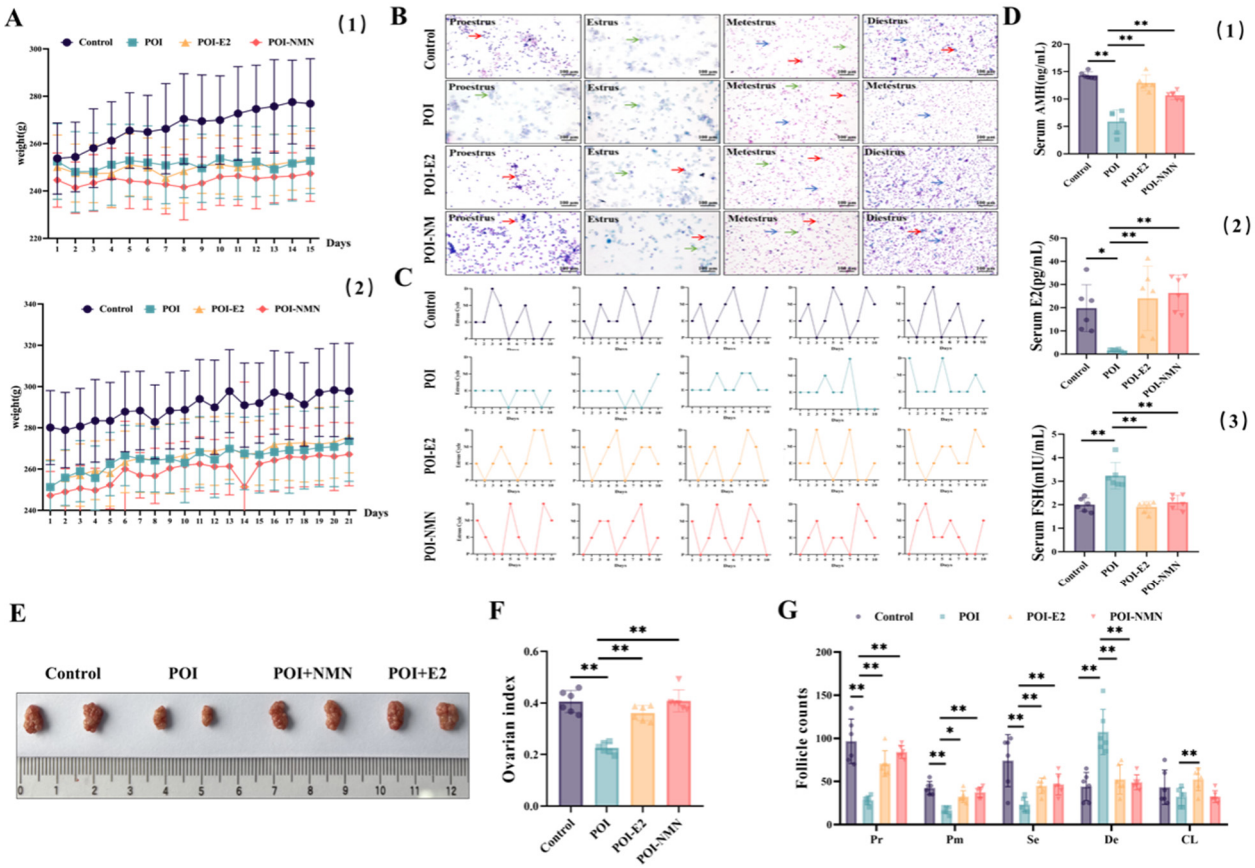

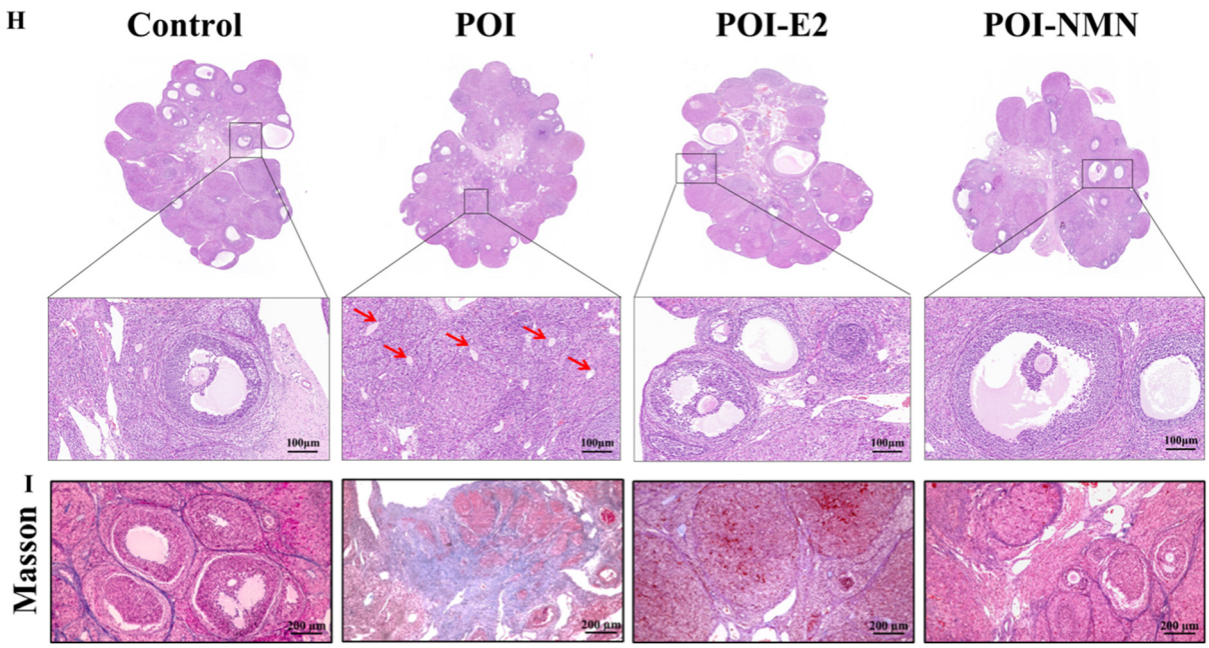

Figure 1 NMN and E2 treatment improved the ovarian reserve function of POI rats A: Body weight of each group (n=10 per group, 8 Weeks). (1) Body weight of the rats during the modeling period，(2) Body weight of the rats 15 days after modeling.B: Cytological assessment of vaginal smears (n=5 per group, day 46-56). Red arrows, nuclear epithelial cells; green arrows, cornified squamous epithelial cells; blue arrows, leucocytes. C: Line chart of estrous cycle (P, proestrus; E, estrous; M, metestrus; D, diestrus).D: Serum concentrations of AMH (1) , E2(2) and FSH(3) (n=6 rats per group). E: Ovarian morphology of each group.F: Ovarian index (ovary/body weight) of each group (n=6 rats per group).G: Counts of cystic follicles and corpus luteum (n=6 per group). H: HE staining scan and magnification of ovarian sections in each group (n=6 per group, scale bar in upper is 100 μm). The lower panel show the higher magnification of the box area in the upper panel respectively.(Red arrows, atretic follicles) I: Masson staining scan and magnification of ovarian sections in each group (n=6 per group, scale bar in upper is 200 μm). Data were presented as mean ± SEM. Significant differences were respectively presented as ns, no significance; $*P < 0.05$; $**P < 0.01$.

Since ovarian function is closely related to steroid hormones, we examined the potential effects of NMN and E2 on ovarian hormone levels. As shown in Figure1D, compared with the control group, the mean serum FSH concentration (3.237 ± 0.5627； n=6) of the POI group increased significantly, while the mean serum AMH (5.857 ± 2.143; n=6) and E2 (1.487 ± 0.6241; n=6) concentrations decreased significantly (Figure1D). Compared with the POI group, the mean concentration of serum FSH (1.898 ± 0.2373; n=6) decreased in the POI-E2 and POI-NMN groups, while the mean concentrations of AMH (12.95 ± 1.443； n=6) and E2 (24.02 ± 13.86； n=6) increased significantly (Figure 1D).

To further confirm the effects of NMN and E2 on ovarian function, the morphology and ovarian reserve function of four groups of rats were compared. As shown in Figure 1E-F, compared with the Control group, the ovarian volume of rats in the POI group decreased (Figure 1E), and the ovarian index (ovary/body weight) decreased ($P < 0.01$) (Figure 1F). Furthermore, as illustrated in Figures 1G-I, we measured the number of follicles at different stages and corpora lutea and assessed the histology of rat ovaries to determine the effects of NMN and E2 on follicular development and ovulation. Compared to the Control group, the number of follicles and corpora lutea at each developmental stage decreased in the POI group, with an increase in the number of atretic follicles (Figure 1G-H), and a severe degree of ovarian fibrosis in the latter (Figure 1I). Under the intervention of NMN and E2, ovarian volume and ovarian index significantly recovered (Figure 1E-H). The number of follicles at different developmental stages significantly increased, and the number of

atretic follicles decreased in the POI-NMN group and POI-E2 group (Figure 1G). The results showed that in CTX-induced POI rats, administration of NMN and E2 gradually regulated the estrous cycle. Serum levels of estradiol and AMH significantly increased, while FSH levels significantly decreased. The ovarian index significantly increased. HE staining revealed that NMN and E2 interventions significantly increased the number of primordial, primary, and secondary follicles, reduced the number of atretic follicles, and effectively improved the degree of ovarian fibrosis.

3.2 NMN restore glycolysis and suppress pyroptosis by enhancing lactate and NAD+ in POI rats

To investigate the effects of NMN and E2 on lactate and NAD^+ levels in the ovaries of POI rats, we measured lactate and NAD^+ concentrations in each group. As shown in Figure 2A and Figure 2B, the levels of lactate and NAD^+ in the ovaries of POI rats significantly decreased, but significantly increased after NMN and E2 intervention(Figure 2A-B). The ovaries, as low-oxygen organs, generate energy for follicular development via glycolysis, with lactate production driven by key enzymes (HK2, PKM2, and LDHA). Here, we examined the expression of these enzymes in the ovaries by Western blotting, qRT-PCR, and immunohistochemistry.

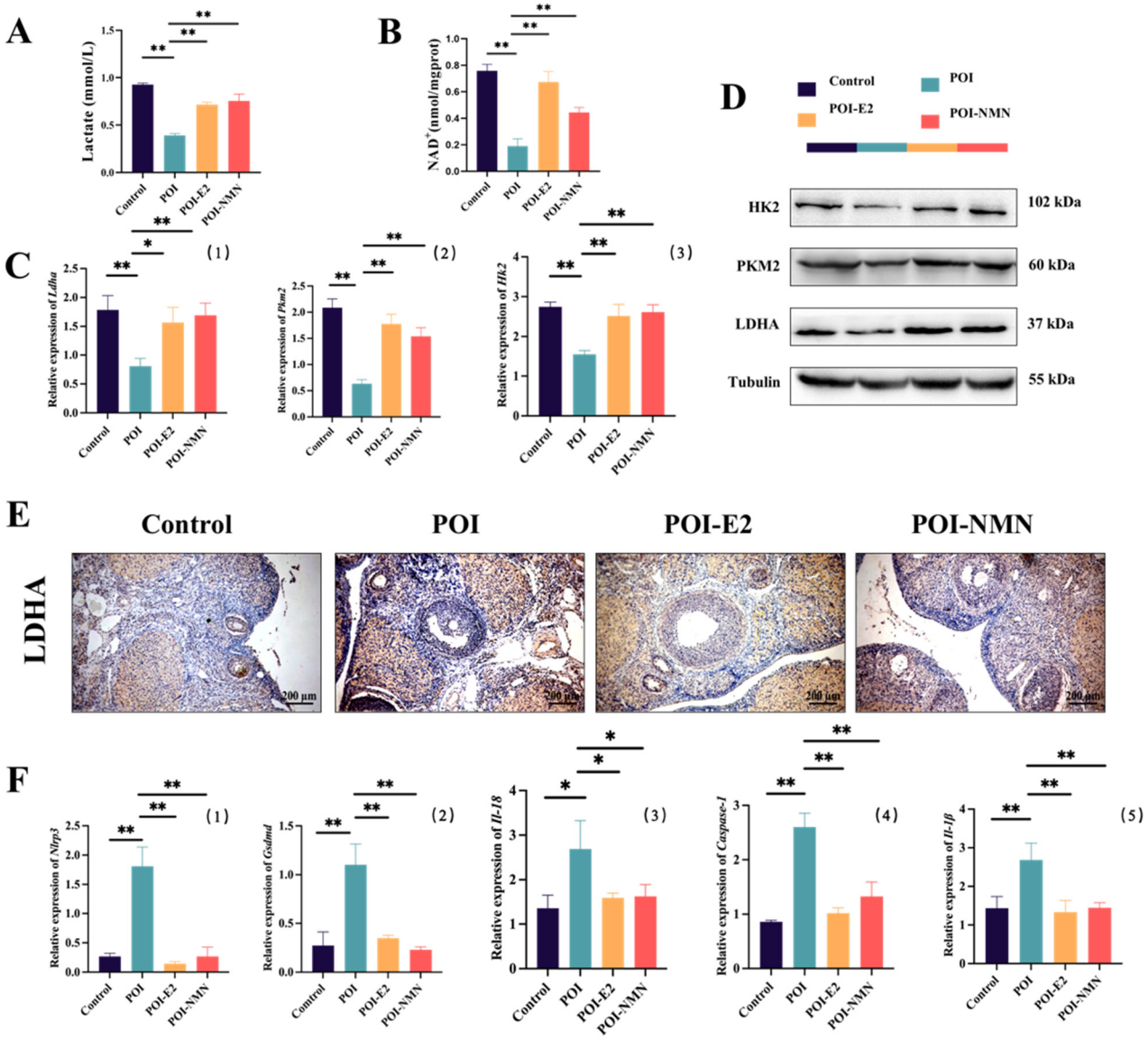

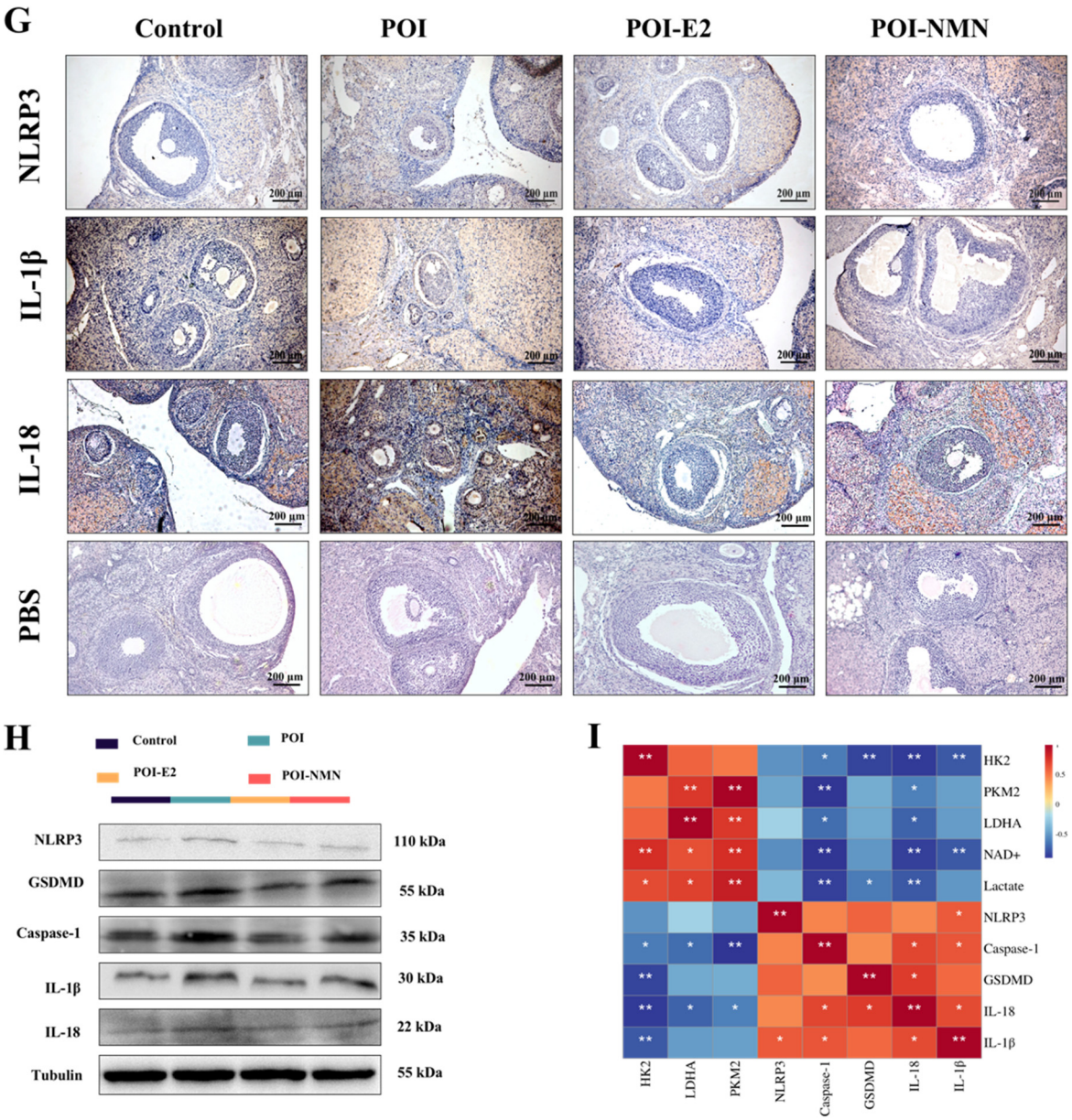

Figure 2 NMN restore glycolysis and suppress pyroptosis by enhancing lactate and NAD^+ in POI rats A: Lactate levels in rat ovaries. B: NAD^+ levels in rat ovaries. C: The expression of LDHA (1), PKM2 (2), HK2 (3) at the mRNA level were detected by qRT-PCR (n=3 per group). D: Western blotting detected the expression of HK2, PKM2, LDHA proteins in rat ovaries of each group. E: Immunohistochemical detection of the expression of LDHA in ovarian tissues. F: The expression changes of NLRP3 (1), GSDMD (2), IL-18 (3) ,IL-1β (4) and Caspase-1 (5) at the mRNA level were detected by qRT-PCR (n=3 per group). G: Immunohistochemical detection of inflammatory factors NLRP3, IL-18 and IL-1β expression in ovarian tissues. H: Western blotting detected the expression of NLRP3, GSDMD, Caspase-1, IL-18 and IL-1β proteins in rat ovaries of each group. I: Correlation analysis of glycolytic rate-limiting enzyme genes LDHA, HK2, PKM2, lactate, and NAD^+ with inflammatory factors IL-18, IL-1β, Caspase-1, GSDMD and NLRP3 senescence factors. Significant differences between groups were indicated as ns, no significance; $*P < 0.05$; $**P < 0.01$. The qRT-PCR analysis showed that compared to the control group, the mRNA expression of HK2, PKM2, and LDHA in POI rats significantly decreased, but the POI-NMN group and POI-E2 exhibited a restoration in the expression of these enzymes (Figure 2C). WB and IHC results confirmed that the protein expression levels of HK2, PKM2 and LDHA in the POI group were reduced compared to the control group, consistent with PCR results. The POI-NMN and POI-E2 groups also showed restoration of the expression of these enzymes (Figure 2D-E).

Interrupting glycolytic flux and reducing lactate levels can induce inflammasome signaling and cell pyroptosis. To investigate the effects of NMN and E2 on granulosa cell pyroptosis in POI rats, we used WB, qRT-PCR, and immunohistochemistry to detect the expression of key factors related to pyroptosis (NLRP3, CASPASE-1, GSDMD, IL-1β, and IL-18).

The qRT-PCR analysis showed that the expression of all pyroptosis factors in the POI group was elevated compared to the control group, but decreased after treatment with NMN and E2 (Figure 2F). Immunohistochemistry results confirmed that the expression of pyroptosis factors in the ovaries of POI rats was significantly upregulated compared to the control group. However, after treatment with NMN and E2, the positive expression of NLRP3, CASPASE-1, GSDMD, IL-1β, and IL-18 showed significant reduction (Figure 2G). The protein expression observed in WB was consistent with the trends observed in qRT-PCR and IHC analysis (Figure 2H).

To understand whether there is a relationship between the glycolytic pathway, lactate, NAD^+, and pyroptosis pathways, we conducted correlation analysis of glycolytic enzymes (HK2, PKM2, and LDHA), lactate, NAD^+, and pyroptosis factors (NLRP3, CASPASE-1, GSDMD, IL-1β, and IL-18) in rats. We found significant correlations among these four factors (Figure 2I), indicating mutual influence between them.

3.3 NMN modulates lactate production to suppress NLRP3-mediated inflammatory aging

Based on the above results, we speculate that NMN may maintain lactate levels in the ovaries of POI rats by increasing NAD^+ levels. Concurrently, it significantly inhibits the expression of inflammatory aging-related factors such as NLRP3, thereby improving the declining ovarian reserve function in POI rats. To further explore its molecular mechanism, we treated KGN cells with different concentration of CTX and measured both cell viability and lactate production levels. The results demonstrated a dose-dependent decrease in both KGN cell viability and lactate generation. Based on these findings, we selected 4 μg/mL CTX for subsequent cellular experiments (Fig. S3A-B). We simulated NLRP3 activation at the cellular level by adding lipopolysaccharide (LPS) and nigericin (Nig) and intervened with NMN to elevate NAD^+ levels in CTX-treated granulosa cells. Results showed that both LPS + Nig and CTX treatments decreased lactate and NAD^+ generation in granulosa cells, while NMN intervention after CTX treatment increased lactate and NAD^+ generation (Figure 3A-B). qRT-PCR and WB results demonstrated downregulation of glycolytic rate-limiting enzyme genes (HK2, PKM2, LDHA) after LPS + Nig and CTX treatments (Figure 3C, E), along with significant upregulation of inflammatory-related genes (NLRP3, GSDMD, CASPASE-1, IL-1β, IL-18) (Figure 3D, F). However, after NMN intervention following CTX treatment, expression of glycolytic rate-limiting enzyme genes increased (Figure 3C, E), and expression of inflammatory-related genes decreased (Figure 3D, F). ELISA results of cell culture supernatants showed a decrease in the secretion of AMH after LPS + Nig and CTX treatments, while secretion increased after NMN intervention following CTX treatment (Figure 3G). Correlation analysis among lactate, NAD^+, glycolytic enzymes (HK2, PKM2, LDHA), and pyroptosis factors (NLRP3, CASPASE-1, GSDMD, IL-1β, IL-18) revealed a significant negative correlation between lactate and NAD^+ levels, expression of glycolytic rate-limiting enzyme genes, and expression of inflammatory aging-related factors (Figure 3H). Taken together, promoting lactate generation can significantly inhibit the expression of inflammatory aging-related factors such as NLRP3, thereby improving the decline in ovarian reserve function.

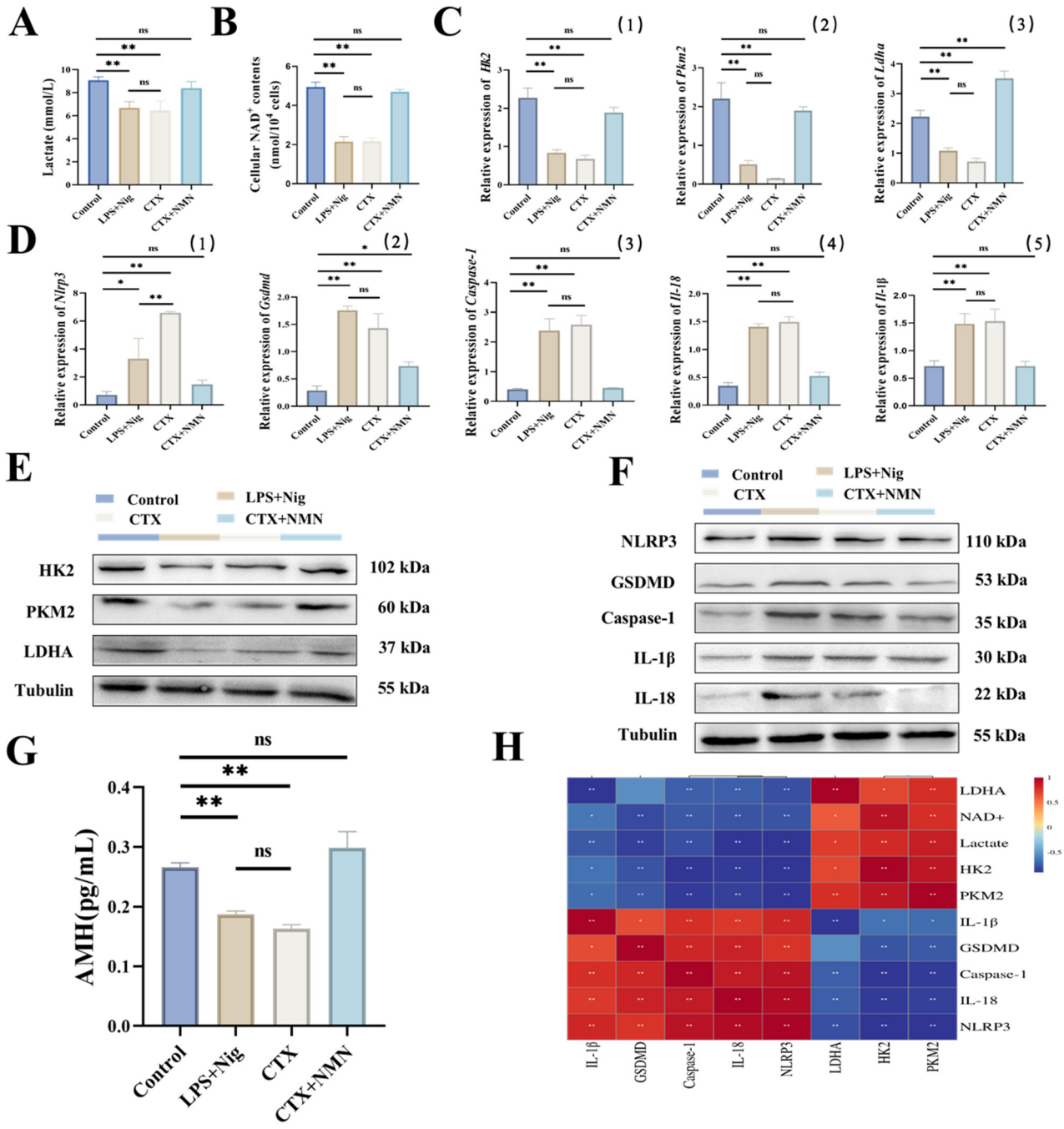

Figure 3 NMN modulates lactate production to suppress NLRP3-mediated inflammatory aging
A: Lactate levels in KGN cells.B: NAD^+ levels in KGN cells.C: The expression of HK2 (1), PKM2 (2), LDHA (3) at the mRNA level were detected by qRT-PCR (n=3 per group). D: The expression of NLRP3 (1), GSDMD (2), Caspase-1 (3), IL-18 (4) and IL-1β (5) at the mRNA level were detected by qRT-PCR (n=3 per group). E: Western blotting detected the expression of HK2, PKM2, LDHA proteins in KGN cells of each group. F: Western blotting detected the expression of NLRP3, GSDMD, Caspase-1, IL-18 and IL-1β proteins in KGN cells of each group. G: ELISA analysis of AMH expression in KGN cells. H: Correlation analysis of glycolytic rate-limiting enzyme genes LDHA, HK2, PKM2, lactate, and NAD^+ with inflammatory factors IL-18, IL-1β, Caspase-1, GSDMD and NLRP3 senescence factors. Significant differences between groups were indicated as ns, no significance; $*P < 0.05$; $**P < 0.01$.

3.4 Regulation of NLRP3 Gene Function by Lactate Production in KGN Cells

To further explore the regulation of lactate levels on the expression of NLRP3-mediated inflammatory related factors, we employed cobalt chloride (CoCl2), 2-deoxy-D-glucose (2-DG), and lactate to treat granulosa cells cultured *in vitro*. The results revealed that cobalt chloride, simulating a low-oxygen environment in follicles, significantly increased the levels of lactate and NAD^+ in granulosa cells (Figure

4A-B). Both qRT-PCR and Western blot results showed an increase in the expression of glycolytic rate-limiting enzyme genes (Figure 4C, E), accompanied by the suppression of NLRP3 activation and a decrease in the expression of related inflammatory factors (Figure 4D, F). ELISA results from cell supernatants showed an increase in AMH secretion (Figure 4G). Similar results were observed upon direct addition of lactate to the cells (Figure 4H-N). However, treatment with 2-DG resulted in decreased expression of glycolytic rate-limiting enzyme genes as shown by qRT-PCR and Western blot (Figure 4J, L), reduced lactate production (Figure 4H), activation of NLRP3, and an increase in the expression of inflammatory factors (Figure 4K, M). ELISA results showed a decrease in AMH secretion (Figure 4N). Correlation analysis demonstrated a significant negative correlation between changes in lactate levels regulated by multiple methods and the expression of inflammatory factors including NLRP3 (Figure 4O-P). In conclusion, these results further confirm the involvement of lactate in regulating NLRP3-mediated inflammaging, which improved ovarian reserve function.

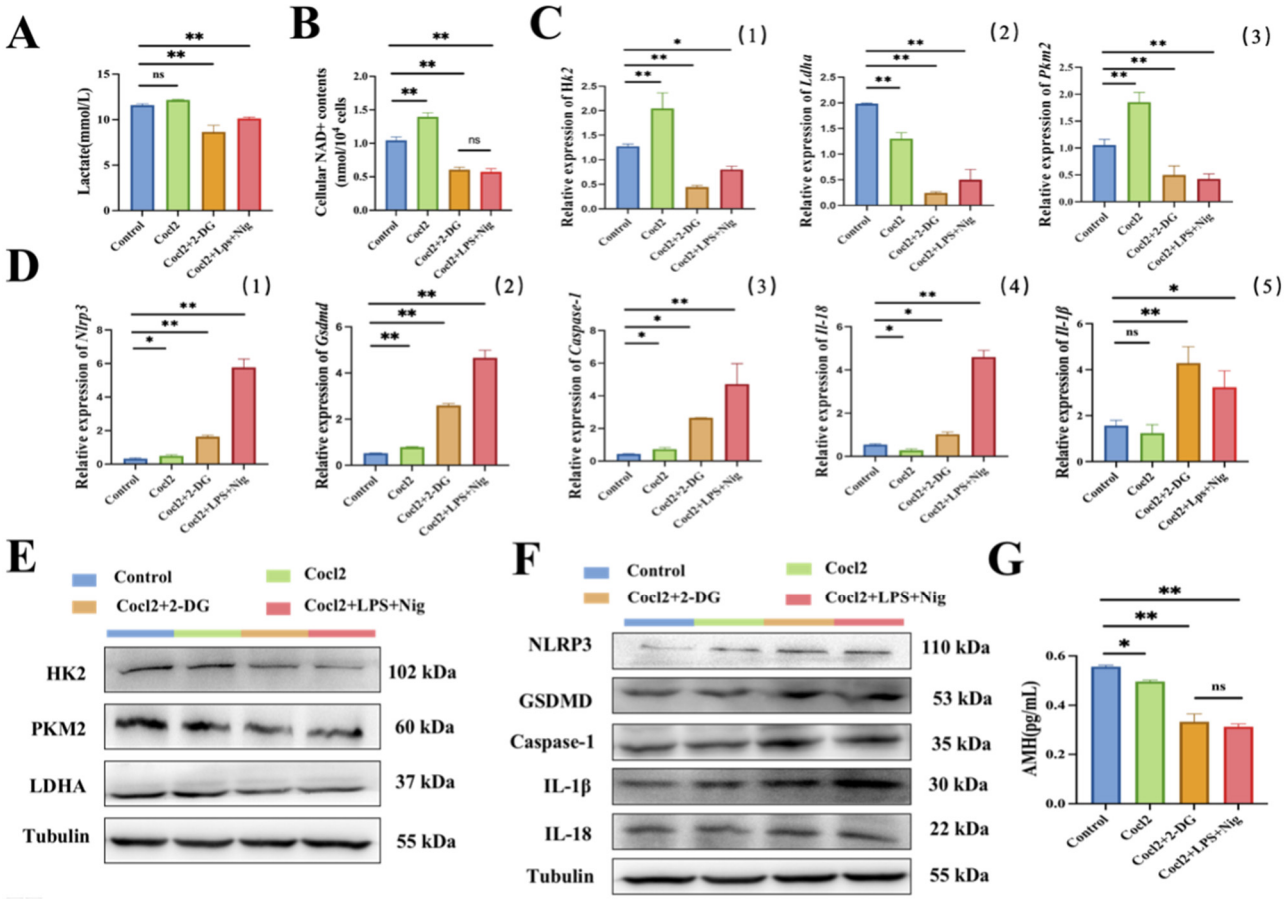

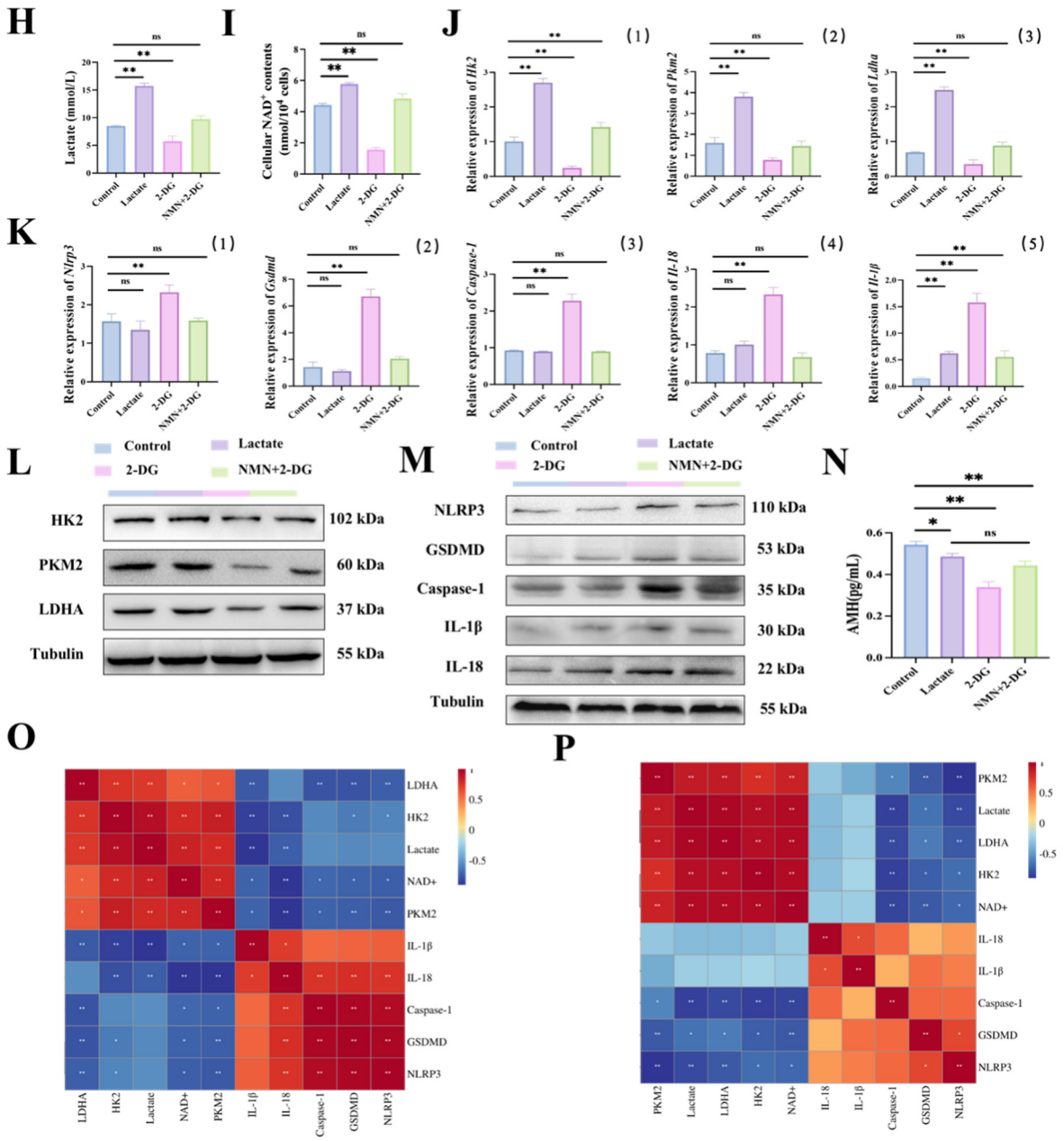

Figure 4 Regulation of NLRP3 Gene Function by Lactate Production in KGN Cells A: Lactate levels in KGN cells. B: NAD^+ levels in KGN cells. C: The expression of HK2 (1), PKM2 (2), LDHA (3) at the mRNA level were detected by qRT-PCR (n=3 per group). D: The expression of NLRP3 (1), GSDMD (2), Caspase-1 (3), IL-18 (4) and IL-1β (5) at the mRNA level were detected by qRT-PCR (n=3 per group). E: Western blotting detected the expression of HK2, PKM2, LDHA proteins in KGN cells of each group. F: Western blotting detected the expression of NLRP3, GSDMD, Caspase-1, IL-18 and IL-1β proteins in KGN cells of each group. G: ELISA analysis of AMH expression in KGN cells. H: Lactate levels in KGN cells. I: NAD^+ levels in KGN cells. J: The expression of HK2 (1), PKM2 (2), LDHA (3) at the mRNA level were detected by qRT-PCR (n=3 per group). K: The expression of NLRP3 (1), GSDMD (2), Caspase-1 (3), IL-18 (4) and IL-1β (5) at the mRNA level were detected by qRT-PCR (n=3 per group). L: Western blotting detected the expression of HK2, PKM2, LDHA proteins in KGN cells of each group. M: Western blotting detected the expression of NLRP3, GSDMD, Caspase-1, IL-18 and IL-1β proteins in KGN cells of each group. N: ELISA analysis of AMH expression in KGN cells. O: Correlation analysis of glycolytic rate-limiting enzyme genes LDHA, HK2, PKM2, lactate, and NAD^+ with inflammatory factors IL-18, IL-1β, Caspase-1, GSDMD and NLRP3 senescence factors. P: Correlation analysis of glycolytic rate-limiting enzyme genes LDHA, HK2, PKM2, lactate, and NAD^+ with inflammatory factors IL-18, IL-1β, Caspase-1, GSDMD and NLRP3 senescence factors. Significant differences between groups were indicated as ns, no significance; $^*P < 0.05$; $^{**}P < 0.01$.

3.5 Lactate regulates the post translational modifications of NLRP3 protein: acetylation and lactylation

To study the levels of protein acetylation and lactylation modifications in the ovaries of rats, we used Pan-Ac antibodies and Pan-Kla antibodies to assess the levels of acetylation and lactylation of ovarian

proteins in POI rats, in conjunction with the lactate levels in the ovaries of these rats (Figure 2). We discovered a negative correlation between acetylation levels and lactate levels, while a positive correlation was observed between lactylation levels and lactate levels (Figure 5A, B). Interestingly, we noted significant variations in acetylation and lactylation levels between 45 kDa and 130 kDa, within which NLRP3 is located. To determine whether NLRP3 undergoes acetylation and acetylation modifications, we transfected Flag-NLRP3 separately into 293T cells. It was found that the acetylation and acetylation levels of NLRP3 were elevated, confirming that NLRP3 can be modified by acetylation and acetylation (Figure 5C). Additionally, we found through molecular docking models that lactate can bind to lysine residues on the NLRP3 protein (Figure 5D), suggesting that lactate may participate in the protein modification of NLRP3, which could affect its activity and function. In 293T cells transfected with Flag-NLRP3, we treated the cells with NALA and the LDHA inhibitor, Oxamate, and then performed immunoprecipitation to detect the acetylation and lactylation levels of NLRP3. Results showed that NALA treatment significantly reduced the acetylation levels of NLRP3 while increasing its lactylation levels, whereas oxamate treatment yielded opposite results (Figure 5E). Consistent with the LDHA inhibitor treatment, knockdown of LDHA by small hairpin RNA (shRNA) also increased NLRP3 acetylation levels while diminishing lactylation levels (Figure 5F). These results indicate that lactate is involved in the acetylation and lactylation modifications of NLRP3.

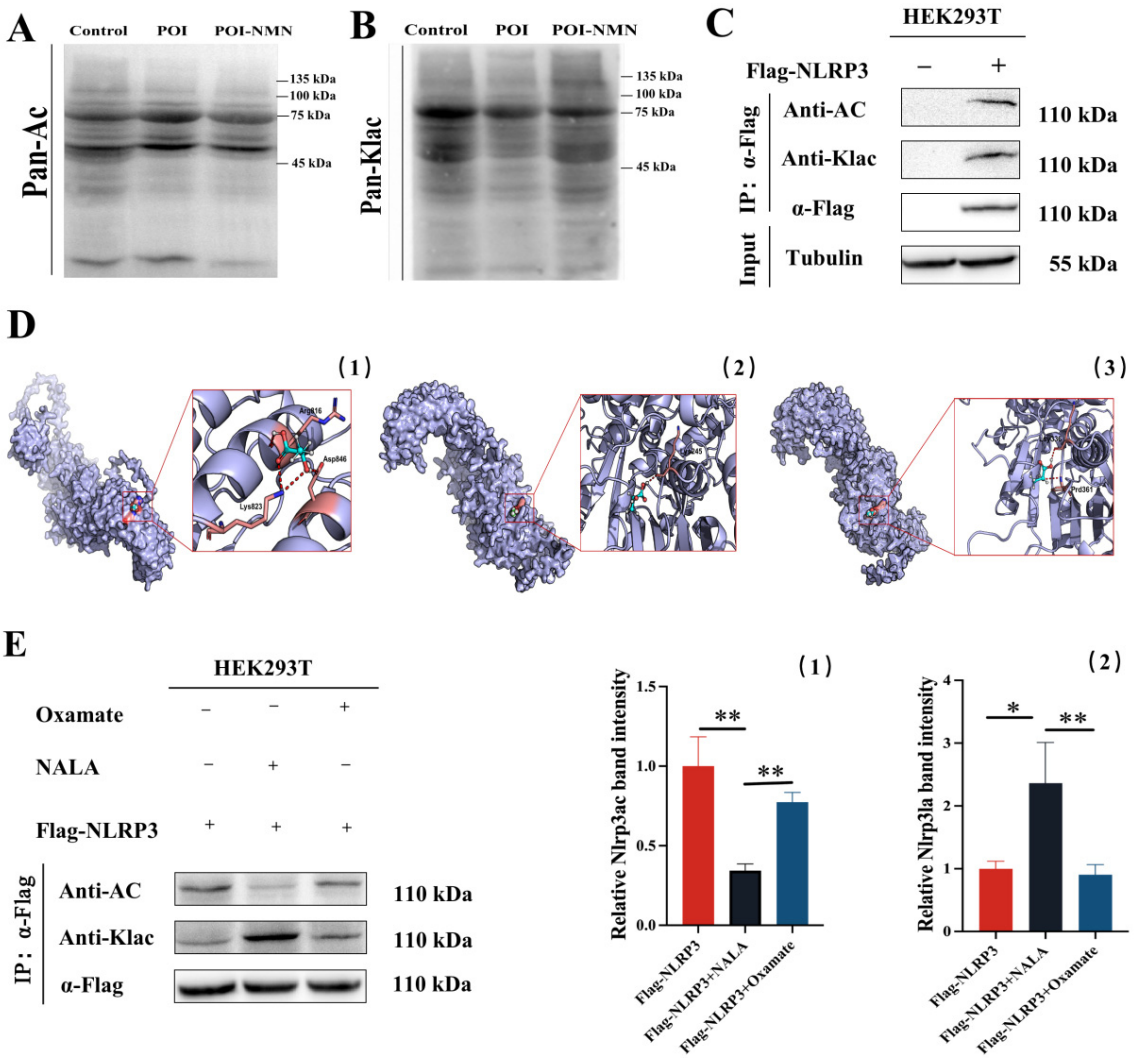

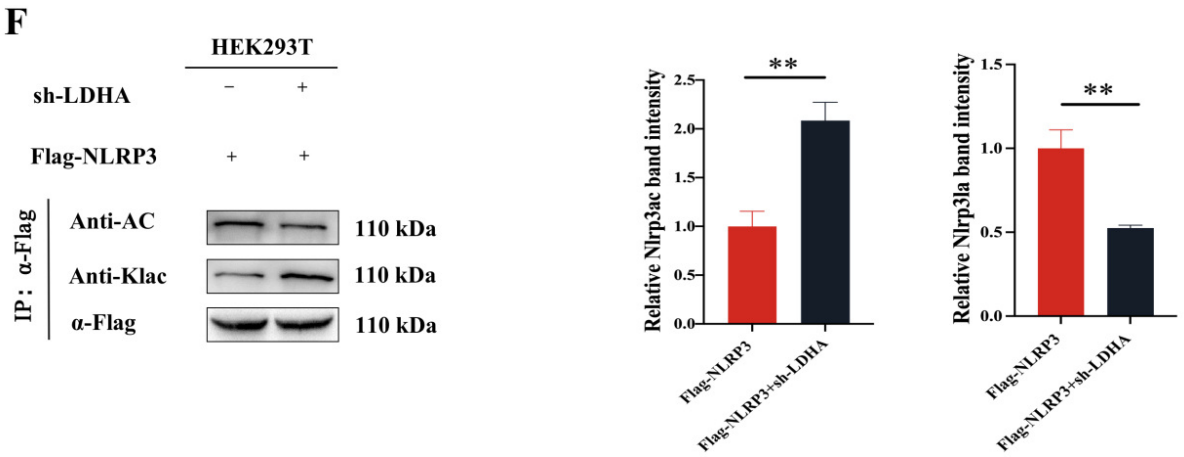

Figure 5 Lactate regulates the post translational modifications of NLRP3 protein: acetylation and lactylation A: The pan-lysine acetylation (Pan-AC) level in rat ovaries of each group were measured by western blot. B: The pan-lysine lactylation (Pan-Kla) level in in rat ovaries of each group were measured by western blot. C: 293T cells were transfected with Flag-NLRP3, and the modifications of NLRP3 acetylation/lactylation were assessed using Pan-AC and Pan-Klac antibodies. D: Molecular docking models were used to simulate the binding sites of lactate with human and rat NLRP3 proteins. E: 293T cells were transfected with Flag-NLRP3 for both the experimental group and the treatment group. The NALA group was treated with 20 mmol/L NALA, and the Oxamate group was treated with 20 mmol/L Oxamate for 24 hours before collecting samples for co-IP experiments. Following protein extraction, Western blotting was performed to determine the levels of NLRP3 acetylation/lactylation modifications. Representative images (left panel) and the quantification (right panel NLRP3ac(1), NLRP3la(2)). F: Co-transfection of 293T cells with Flag-NLRP3 and specific shLDHA plasmids. Co-IP and Western blotting to detect the acetylation/lactylation levels of NLRP3. Representative images (left panel) and the quantification (right panel NLRP3ac(1), NLRP3la(2)). Data were presented as mean ± SEM. Significant differences were respectively presented as ns, no significance; $*P < 0.05$; $**P < 0.01$.

3.6 Verification of key modifying enzymes and sites for NLRP3 acetylation

Given that protein modifications of NLRP3 play an important role in the inflammatory response, we aimed to elucidate the regulatory mechanisms of NLRP3 acetylation. First, we focused on determining the enzymatic mechanisms of NLRP3 acetylation. To identify the deacetylases of NLRP3, we transfected Flag-NLRP3 into 293T cells and treated them with the deacetylase inhibitors NAM (a SIRT family inhibitor) and TSA (an HDAC inhibitor). We observed that the acetylation level of NLRP3 increased upon addition of the SIRT family inhibitor NAM, indicating that the SIRT family participates in the regulation of NLRP3 acetylation (Figure S1A). Then, we co-expressed Flag-NLRP3 with SIRT1-7 in 293T cells and found that only the expression of SIRT3 significantly reduced the acetylation level of NLRP3 (Figure S1B-C). Furthermore, through immunoprecipitation, we found that NLRP3 can co-precipitate with SIRT3 (Figure 6A). Similarly, knockdown of SIRT3 using shRNA increased the acetylation level of NLRP3 (Figure 6B), confirming SIRT3 as the deacetylase of NLRP3.

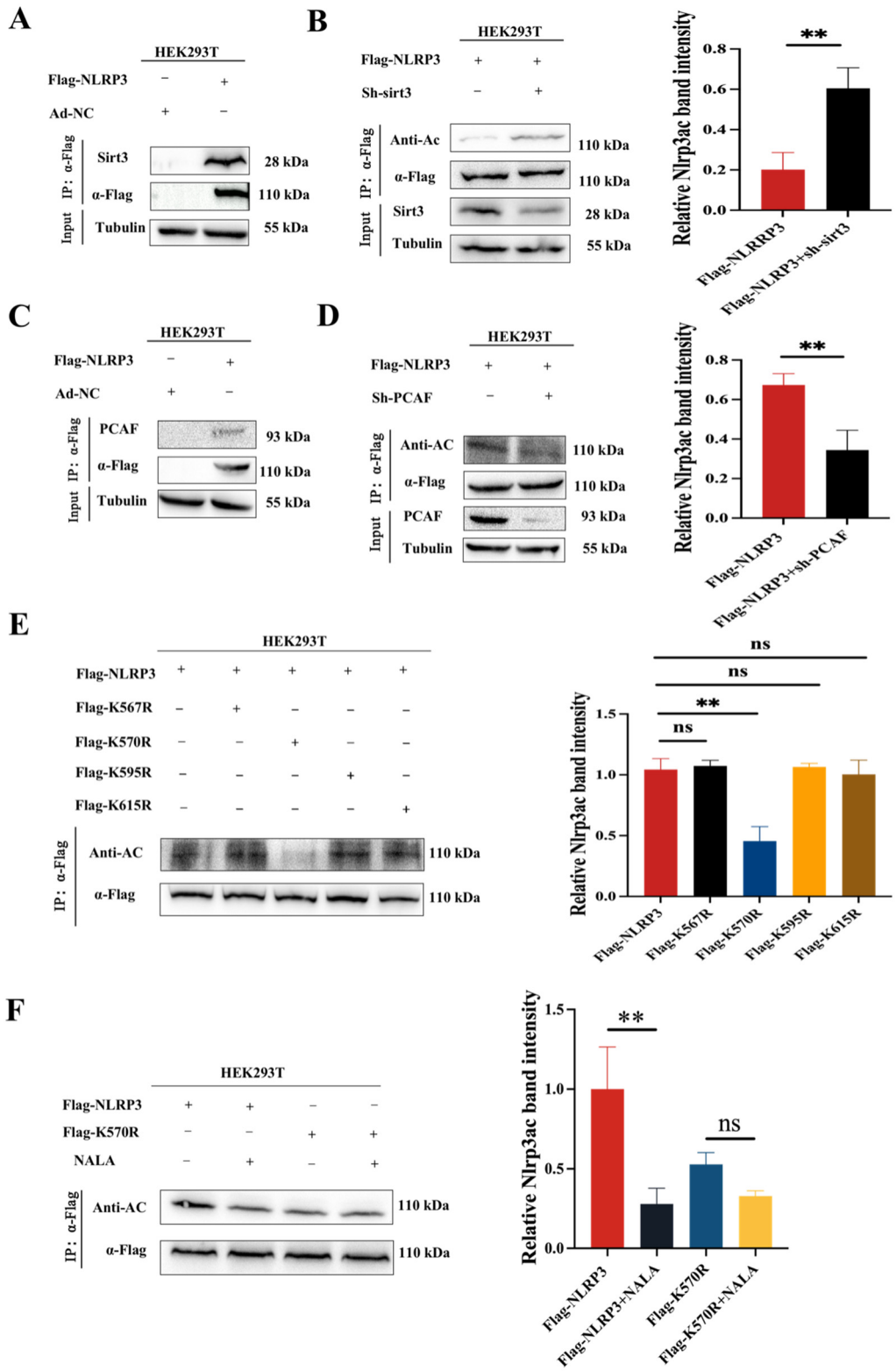

Figure 6 Verification of key modifying enzymes and sites for NLRP3 acetylation A: Co-IP and Western blotting to examine the interaction between NLRP3 and SIRT3. B: Co-transfection of 293T cells with Flag-NLRP3 and specific shSIRT3 plasmids. Co-IP and Western blotting to detect the acetylation levels of NLRP3. Representative images (left panel) and the quantification (right panel). C: Co-IP and Western blotting to examine the interaction between NLRP3 and PCAF. D: Co-transfection of 293T cells with Flag-NLRP3 and specific shPCAF plasmids. Co-IP and Western blotting to detect the acetylation levels of NLRP3. Representative images (left panel) and the quantification (right panel). E: K567R, K570R, K595R and K615R mutant plasmids were transfected into 293T cells, and the protein acetylation levels were detected by Western blotting. Representative images (left panel) and the quantification (right panel). F: 293T cells were transfected with Flag-NLRP3 or Flag-K570R, treated with or without NALA, Co-IP and Western blotting to detect the acetylation levels of NLRP3. Representative images (left panel) and the quantification (right panel). Data were presented as mean ± SEM. Significant differences were respectively presented as ns, no significance; *$P < 0.05$; **$P < 0.01$.

Next, we identified the acetyltransferase of NLRP3. We co-transfected Flag-NLRP3 with four acetyltransferases in 293T cells: GCN5 (KAT2A), PCAF (P300/CBP-associated factor, also known as KAT2B), cAMP response element-binding protein (CREB)-binding protein (CBP), and P300 (E1A binding protein, 300 kDa).[30] We found that PCAF increased NLRP3 acetylation, while the other acetyltransferases had little to no effect (Figure S1D-E). Additionally, immunoprecipitation showed that NLRP3 can co-precipitate with PCAF (Figure 6C), and knockdown of PCAF using shRNA reduced NLRP3 acetylation (Figure 6D), confirming PCAF as the acetyltransferase for NLRP3. To further explore the functional sites of NLRP3 acetylation modification， we performed mass spectrometry to identify potential acetylation sites on NLRP3 . We constructed NLRP3 mutants with lysine to arginine substitutions at these sites and evaluated their acetylation levels in 293T cells. We observed that mutation at the K570 site resulted in a significant decrease in acetylation levels (Figure 6E). Under NALA treatment conditions, there was no significant change in NLRP3 acetylation levels (Figure 6F), indicating that the lysine at position 570 may be a key regulatory site for NLRP3 acetylation.

3.7 Verification of key modifying enzymes and sites for NLRP3 lactylation

To identify the delactylase of NLRP3, we used NAM and TSA to determine whether SIRT or HDAC was involved in NLRP3 delactylation. We found that treatment with the SIRT inhibitor NAM increased NLRP3 lactylation in 293T cells transfected with Flag-NLRP3, indicating that members of the SIRT family preferentially participate in NLRP3 delactylation (Figure S2A). Among SIRT1-7, only the expression of SIRT2 significantly reduced the lactylation level of NLRP3 (Figure S2B-C), and co-immunoprecipitation showed that NLRP3 can co-precipitate with SIRT2 (Figure 7A). Furthermore, knockdown of SIRT2 using shRNA resulted in increased NLRP3 lactylation levels (Figure 7B), confirming SIRT2 as the de-lactylase for NLRP3.

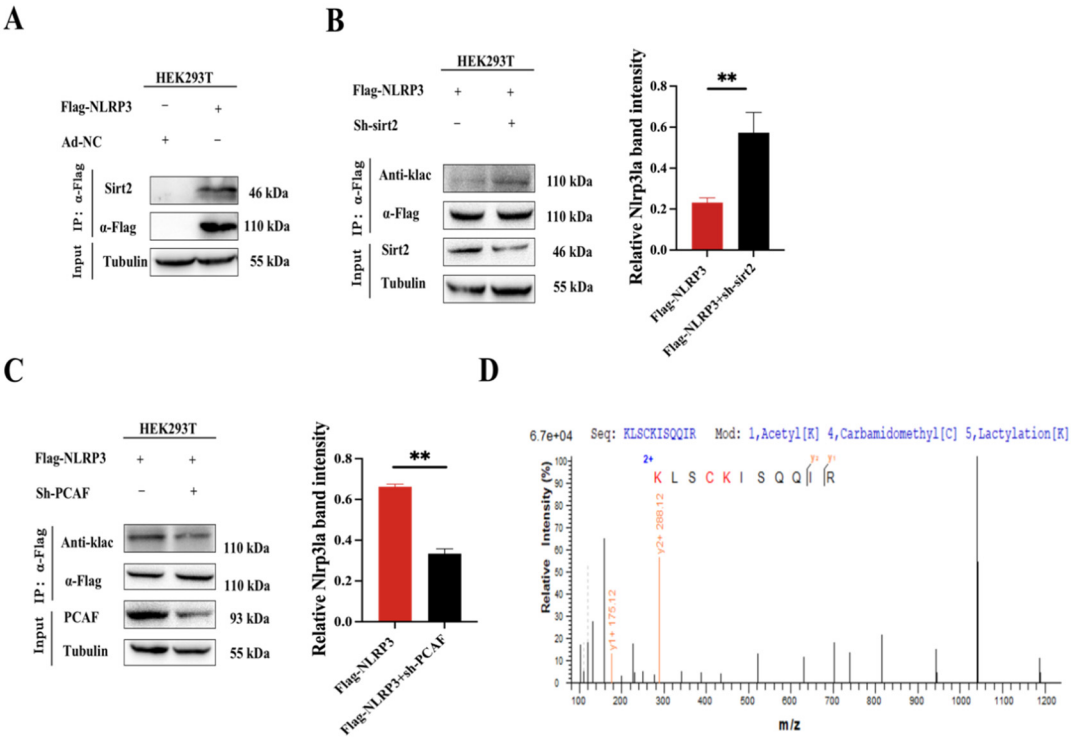

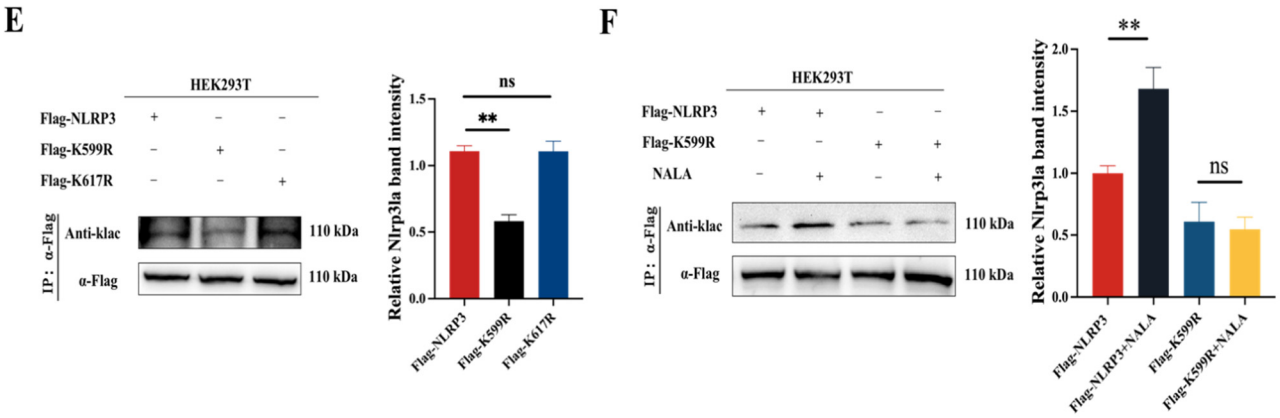

Figure 7 Verification of key modifying enzymes and sites for NLRP3 lactylation A: Co-IP and Western blotting to examine the interaction between NLRP3 and SIRT2. B: Co-transfection of 293T cells with Flag-NLRP3 and specific shSIRT2 plasmids. Co-IP and Western blotting to detect the lactylation levels of NLRP3. Representative images (left panel) and the quantification (right panel). C: Co-transfection of 293T cells with Flag-NLRP3 and specific shPCAF plasmids. Co-IP and Western blotting to detect the lactylation levels of NLRP3. Representative images (left panel) and the quantification (right panel). D: Mass spectrometry analysis revealed potential lactylation sites in NLRP3. E: K599R and K617R mutant plasmids were transfected into 293T cells, and the protein lactylation levels were detected by Western blotting. Representative images (left panel) and the quantification (right panel). F: 293T cells were transfected with Flag-NLRP3 or Flag-K599R, treated with or without NALA, Co-IP and Western blotting to detect the lactylation levels of NLRP3. Representative images (left panel) and the quantification (right panel). Data were presented as mean ± SEM. Significant differences were respectively presented as as ns, no significance; $^{*}P < 0.05$; $^{**}P < 0.01$.

To identify the lactylase of NLRP3, we also examined four acetyltransferases: GCN5, PCAF, CBP, and P300. We found that only PCAF increased NLRP3 lactylation, while the other acetyltransferases had little to no effect (Figure S2D-E). Additionally, knockdown of PCAF reduced the lactylation level of NLRP3 (Figure 7C), confirming that PCAF is also a lactylase for NLRP3. Mass spectrometry identified potential lactylation sites on NLRP3 (Figure 7D), and we mutated two presumed lactylation sites to arginine (R) and assessed their lactylation levels. The results showed that the mutation at the K599 site significantly decreased lactylation levels (Figure 7E). Under NALA treatment conditions, there was no significant change in NLRP3 acetylation levels(Figure 7F), indicating that the lysine at position 599 may be a key regulatory site for NLRP3 lactylation.

3.8 Lactate regulates the inflammatory factors in KGN cells

The preceding discussion suggests that lactate can influence the protein function and activity of NLRP3 by regulating its acetylation and lactylation. It remains to be explored whether lactate stimulation will still affect the downstream inflammatory factor changes in NLRP3 after modifications at the acetylation and lactylation sites are altered. Therefore, we overexpressed NLRP3, NLRP3-K570R, and NLRP3-K599R in KGN cells and treated them with NALA. The results showed that overexpression of NLRP3 significantly increased the levels of its downstream inflammatory factors IL-1β and IL-18 while decreasing the expression level of AMH, which was restored after NALA treatment. Interestingly, similar to the NLRP3 overexpression group, IL-1β and IL-18 levels were also significantly increased in K599R mutant cells, with a decrease in AMH levels. In contrast, IL-1β and IL-18 levels were significantly decreased in K570R mutant cells, while AMH levels increased. However, we found that adding NALA had little effect on the protein levels of IL-1β, IL-18, and AMH in K599R and K570R mutant cells (Figure 8).

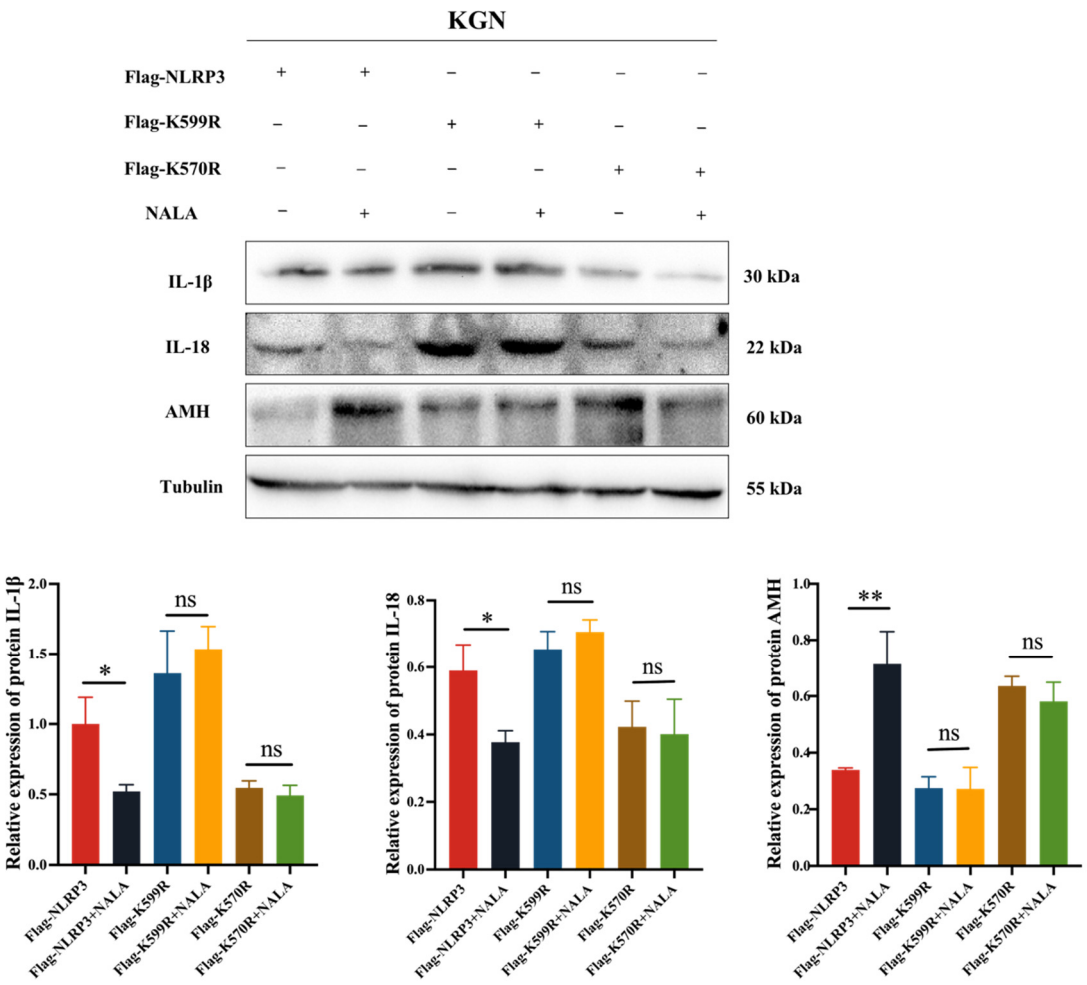

Figure 8 Lactate regulates the inflammatory factors in KGN cells Western blotting detected the expression of IL-1β, IL-18 and AMH proteins in KGN cells of each group. Representative images (up panel) and the quantification (down panel). Data were presented as mean ± SEM. Significant differences were respectively presented as ns, no significance; *$P < 0.05$; **$P < 0.01$.

4. Discussion

POI is characterized by decreased ovarian reserve and hormonal imbalances, serving as the primary cause of female infertility. In this study, we established a cyclophosphamide (CTX)-induced POI rat model, showing ovarian morphological, histological changes and hormone level alterations consistent with clinical POI indicators[1]. Multiple studies have demonstrated that decreased ovarian reserve are closely associated with inflammatory senescence, and many anti-aging strategies are predicated on anti-inflammatory interventions.[31, 32] NLRP3, a pro-inflammatory factor playing a critical regulatory role in various inflammatory senescence-related diseases, is activated to release pro-inflammatory substances IL-1β and IL-18, causing pyroptosis in granulosa cells, which represents a novel mechanism underlying ovarian failure and follicular dysfunction.[33] In this study, we observed that inflammatory senescence factors, such as Nod-like receptor protein 3 (NLRP3), caspase-1, interleukin-1β (IL-1β), and interleukin-18 (IL-18), were significantly elevated in the ovaries of POI rats. This result is consistent with the expression pattern of granulocytes in POI patients.[34] It has been reported that treatments such as metformin, cnidium monnieri extract, acupuncture, and moxibustion can inhibit NLRP3 activation, reduce the expression of IL-1β and IL-18 in ovarian tissue, elevate serum AMH levels, and improve endocrine disorders and ovarian function in rats

with decreased ovarian reserve due to POI.[35, 36] Therefore, inhibiting NLRP3 activity may be crucial for improving ovarian reserve function in POI.

Follicular differentiation and oocyte development primarily rely on the intercellular communication between oocytes and GCs.[37] GCs provide energy substrates to oocytes through gap junction communication, with lactate being a key intermediate product generated from glucose via glycolysis.[38] As initial targets exposed to chemotherapeutic agents, GCs are significantly affected during chemotherapy.[39] Specifically, CTX substantially depletes ovarian granulosa cells, leading to a marked reduction in lactate supply necessary for follicular development and resulting in ovarian function loss.[40] In this study, we observed that key rate-limiting enzymes of glycolysis (LDHA, PKM2, and HK2) were significantly downregulated in both the ovaries of POI rats treated with CTX and in cultured granulosa cells, accompanied by a notable decrease in lactate levels. This finding may elucidate the underlying mechanisms for decreased ovarian reserve function.

NMN, an orally bioavailable NAD+ precursor, is naturally present in foods such as beef, edamame, shrimp, broccoli, and cucumber.[41] It shows potential benefits in retarding aging and improving metabolic health.[42] In our study, the dosage used in rats was 500 mg/kg. Converting this to a human equivalent dose (HED) based on body surface area, we derived an approximate value of 8 mg/kg. For a 50–60 kg adult, this translates to 300–400 mg per day, which aligns with the dosage range of current clinical trials.[43] Interestingly, our study revealed that NMN intervention significantly elevated lactate levels, decreased the expression of inflammatory senescence-related factors such as NLRP3, and increased serum AMH levels, mirroring the clinical effects of E2 in enhancing ovarian reserve function.[44] Previous studies have highlighted a potential relationship between glycolysis and inflammation, suggesting that impaired glycolysis may drive NLRP3-dependent inflammation. When lactate levels significantly decline due to suppressed glycolytic processes, the levels of various inflammatory factors (including NLRP3 and IL-1β) increase markedly.[10] Conversely, lactate supplementation can restore glycolysis and suppress inflammation.[45] Our research demonstrates that NMN can maintain lactate production levels by elevating NAD^+ in ovarian and granulosa cells while significantly inhibiting the expression of inflammatory senescence-related factors such as NLRP3. Additionally, lactate serves as an antioxidant, mitigating oxidative stress-induced cellular damage and subsequently suppressing inflammatory responses.[46] Through modulation of extracellular lactate production, we found a significant negative correlation between lactate levels and the expression of inflammatory senescence factors like NLRP3. Thus, lactate can inhibit NLRP3-mediated inflammatory senescence in granulosa cells, thereby improving ovarian reserve function in POI.

While our findings highlight the role of glycolysis-lactate signaling in NMN-mediated ovarian protection, we cannot exclude the involvement of alternative NAD+-dependent pathways. For instance, NAD+ acts as a co-substrate for sirtuins, which regulate genomic stability and mitochondrial function in ovarian granulosa cells.[47] Additionally, NAD+-dependent PARP1 protects against CTX-induced DNA damage—a process potentially relevant to POI pathogenesis[48]. Future studies could employ pathway-specific inhibitors to dissect the relative contributions of these mechanisms.

Recent studies have reported that lactate acts as an energy substrate,[49] anti-inflammatory agent,[46] and key signaling molecule for protein post-translational modifications (PTMs).[50] Acetylation of NLRP3, a conserved activation switch, promotes release of IL-1β and IL-18.[51] This study reveals lactate inhibits NLRP3 acetylation and, for the first time, demonstrates NLRP3 lactylation—with lactic acid enhancing its lactylation levels. Mechanistically, lactate may suppress inflammation by modulating these modifications. Histone H3K18 shows competitive balance between lactylation and acetylation,[52] but whether NLRP3 exhibits similar competition remains unclear. Some studies have reported that lactate-driven lactylation has been linked to anti-inflammatory effects in Alzheimer's disease[53] and macrophage polarization,[54] which correlates with enhanced lactylation.[55] Our findings suggest lactate mediates NLRP3 acetylation/lactylation to inhibit inflammation, though the regulatory crosstalk between these PTMs requires further study.

PTMs are dynamically regulated by specific 'writer' and 'eraser' enzymes that add or remove modifications to ensure precise cellular signaling.[27] Our investigation revealed that SIRT family proteins, beyond their known deacetylation activity, also possess de-lactylation capabilities. Through comparative studies using HDAC inhibitor TSA and SIRT inhibitor NAM, we identified SIRT3 as the deacetylase and SIRT2 as the de-lactylase for NLRP3. Interestingly, PCAF was found to mediate both acetylation and lactylation of NLRP3, though additional regulatory factors likely contribute to these modifications. While previous work showed KAT5-mediated acetylation at K24 activates NLRP3 in macrophages,[51] our mass spectrometry analysis of KGN cells identified a distinct acetylation site at K570, suggesting cell-type specific regulation.[56, 57] Importantly, we discovered NLRP3 lactylation at K599 - a novel finding demonstrating NLRP3's susceptibility to this modification. Functional studies confirmed that mutation of either K570 or K599 abrogates lactate's ability to regulate downstream inflammatory factors and improve ovarian reserve function, establishing these sites as potential therapeutic targets for POI.

Several limitations should be considered in this study. While our rat model of CTX-induced POI recapitulates key pathological features of human POI, important interspecies differences in ovarian physiology may affect the translational potential of our findings[58, 59]. Specifically: (1) Rat reproductive cycles and hormonal regulation differ substantially from humans, and (2) the CTX-induced model cannot fully capture the multifactorial etiology (e.g., genetic, autoimmune) or sociobehavioral influences of clinical POI. Future studies using non-human primates or human ovarian organoids will be essential to validate NMN's therapeutic efficacy before clinical application.

In summary, our study suggests that NLRP3-mediated inflammation plays a critical role in the pathogenesis of POI, and that lactate supplementation or increased lactate production can lead to NLRP3 inactivation. Increasing intracellular lactate levels has been shown to promote lactylation and inhibit acetylation of NLRP3, thereby reducing cell inflammation and enhancing ovarian reserve function. Moreover, our findings identify PCAF, SIRT2, and SIRT3 as regulatory factors for the acetylation and lactylation of NLRP3. The primary acetylation modification site on NLRP3 is K570, while the main lactylation

modification site is K599. Consequently, targeting these modifications of NLRP3 may offer a potential treatment strategy for POI.

Conflicts of interest

The authors declare no competing interests.

Date availability statement

The data that support the findings of this study are available from the corresponding author upon reasonable request.

Funding

This work was supported by National Natural Science Fund of China (No. 82101720);

The Natural Science Foundation of Guangxi in China (2025GXNSFAA069209); The Hunan Province Innovation and Entrepreneurship Training Program for College Students (No. D202405232106468626).

Acknowledgments

Not applicable.

References

[1] R. European Society for Human, P.O.I. Embryology Guideline Group on, L. Webber, et al., ESHRE Guideline: management of women with premature ovarian insufficiency, Hum Reprod. 31 (2016) 926-937. https://doi.org/10.1093/humrep/dew027.

[2] S. Golezar, F. Ramezani Tehrani, S. Khazaei, et al., The global prevalence of primary ovarian insufficiency and early menopause: a meta-analysis, Climacteric. 22 (2019) 403-411. https://doi.org/10.1080/13697137.2019.1574738.

[3] H. Ke, S. Tang, T. Guo, et al., Landscape of pathogenic mutations in premature ovarian insufficiency, Nat Med. 29 (2023) 483-492. https://doi.org/10.1038/s41591-022-02194-3.

[4] M. De Vos, P. Devroey, B.C. Fauser, Primary ovarian insufficiency, Lancet. 376 (2010) 911-921. https://doi.org/10.1016/S0140-6736(10)60355-8.

[5] J.M. Navarro-Pando, E. Alcocer-Gomez, B. Castejon-Vega, et al., Inhibition of the NLRP3 inflammasome prevents ovarian aging, Sci Adv. 7 (2021) https://doi.org/10.1126/sciadv.abc7409.

[6] J. Fu, H. Wu, Structural Mechanisms of NLRP3 Inflammasome Assembly and Activation, Annu Rev Immunol. 41 (2023) 301-316. https://doi.org/10.1146/annurev-immunol-081022-021207.

[7] G. Reato, L. Morlin, S. Chen, et al., Premature ovarian failure in patients with autoimmune Addison's disease: clinical, genetic, and immunological evaluation, J Clin Endocrinol Metab. 96 (2011) E1255-1261. https://doi.org/10.1210/jc.2011-0414.

[8] C.R. Zhang, W.N. Zhu, W. Tao, et al., Moxibustion against Cyclophosphamide-Induced Premature Ovarian Failure in Rats through Inhibiting NLRP3-/Caspase-1-/GSDMD-Dependent Pyroptosis, Evid Based Complement Alternat Med. 2021 (2021) 8874757. https://doi.org/10.1155/2021/8874757.

[9] S. Shiratsuki, T. Hara, Y. Munakata, et al., Low oxygen level increases proliferation and metabolic changes in bovine granulosa cells, Mol Cell Endocrinol. 437 (2016) 75-85. https://doi.org/10.1016/j.mce.2016.08.010.

[10] L.E. Sanman, Y. Qian, N.A. Eisele, et al., Disruption of glycolytic flux is a signal for inflammasome signaling and pyroptotic cell death, Elife. 5 (2016) e13663. https://doi.org/10.7554/eLife.13663.

[11] N. Xie, L. Zhang, W. Gao, et al., NAD(+) metabolism: pathophysiologic mechanisms and therapeutic potential, Signal Transduct Target Ther. 5 (2020) 227. https://doi.org/10.1038/s41392-020-00311-7.

[12] H. Nadeeshani, J. Li, T. Ying, et al., Nicotinamide mononucleotide (NMN) as an anti-aging health product - Promises and safety concerns, J Adv Res. 37 (2022) 267-278. https://doi.org/10.1016/j.jare.2021.08.003.

[13] K. Liu, H. Wei, W. Nong, et al., Nampt/SIRT2/LDHA pathway-mediated lactate production regulates follicular dysplasia in polycystic ovary syndrome, Free Radic Biol Med. 225 (2024) 776-793. https://doi.org/10.1016/j.freeradbiomed.2024.10.312.

[14] X. Li, Y. Yang, B. Zhang, et al., Lactate metabolism in human health and disease, Signal Transduct Target Ther. 7 (2022) 305. https://doi.org/10.1038/s41392-022-01151-3.

[15] W. Shi, T.J. Cassmann, A.V. Bhagwate, et al., Lactic acid induces transcriptional repression of macrophage inflammatory response via histone acetylation, Cell Rep. 43 (2024) 113746. https://doi.org/10.1016/j.celrep.2024.113746.

[16] Y. Zhang, L. Luo, X. Xu, et al., Acetylation is required for full activation of the NLRP3 inflammasome, Nature Communications. 14 (2023) https://doi.org/10.1038/s41467-023-44203-0.

[17] A.N. Zhao, Z. Yang, D.D. Wang, et al., Disturbing NLRP3 acetylation and inflammasome assembly inhibits androgen receptor-promoted inflammatory responses and prostate cancer progression, The FASEB Journal. 36 (2022) https://doi.org/10.1096/fj.202200673RRR.

[18] K. Yang, M. Fan, X. Wang, et al., Lactate promotes macrophage HMGB1 lactylation, acetylation, and exosomal release in polymicrobial sepsis, Cell Death Differ. 29 (2022) 133-146. https://doi.org/10.1038/s41418-021-00841-9.

[19] J. Zhou, L. Zhang, J. Peng, et al., Astrocytic LRP1 enables mitochondria transfer to neurons and mitigates brain ischemic stroke by suppressing ARF1 lactylation, Cell Metab. 36 (2024) 2054-2068 e2014. https://doi.org/10.1016/j.cmet.2024.05.016.

[20] D.O. Gaffney, E.Q. Jennings, C.C. Anderson, et al., Non-enzymatic Lysine Lactoylation of Glycolytic Enzymes, Cell Chem Biol. 27 (2020) 206-213 e206. https://doi.org/10.1016/j.chembiol.2019.11.005.

[21] J. Wang, Y. Cui, Z. Yu, et al., Brain Endothelial Cells Maintain Lactate Homeostasis and Control Adult Hippocampal Neurogenesis, Cell Stem Cell. 25 (2019) 754-767 e759. https://doi.org/10.1016/j.stem.2019.09.009.

[22] S. Sun, X. Xu, L. Liang, et al., Lactic Acid-Producing Probiotic Saccharomyces cerevisiae Attenuates Ulcerative Colitis via Suppressing Macrophage Pyroptosis and Modulating Gut Microbiota, Front Immunol. 12 (2021) 777665. https://doi.org/10.3389/fimmu.2021.777665.

[23] Y. Ma, W. Nong, O. Zhong, et al., Nicotinamide mononucleotide improves the ovarian reserve of POI by inhibiting NLRP3-mediated pyroptosis of ovarian granulosa cells, J Ovarian Res. 17 (2024) 236. https://doi.org/10.1186/s13048-024-01534-w.

[24] Y. Tang, Y. He, X. Huo, et al., hUMSC-derived exosomes alleviate follicular interstitial cell autophagy by let-7a-5p/AMPK/mTOR axis in POI rats, Stem Cell Res Ther. 16 (2025) 291. https://doi.org/10.1186/s13287-025-04396-1.

[25] C. Han, Y. Yang, Q. Guan, et al., New mechanism of nerve injury in Alzheimer's disease: beta-amyloid-induced neuronal pyroptosis, J Cell Mol Med. 24 (2020) 8078-8090. https://doi.org/10.1111/jcmm.15439.

[26] N.K. Rana, P. Singh, B. Koch, CoCl(2) simulated hypoxia induce cell proliferation and alter the expression pattern of hypoxia associated genes involved in angiogenesis and apoptosis, Biol Res. 52 (2019) 12. https://doi.org/10.1186/s40659-019-0221-z.

[27] F. Li, W. Si, L. Xia, et al., Positive feedback regulation between glycolysis and histone lactylation drives oncogenesis in pancreatic ductal adenocarcinoma, Mol Cancer. 23 (2024) 90. https://doi.org/10.1186/s12943-024-02008-9.

[28] H. Chen, Y. Li, H. Li, et al., NBS1 lactylation is required for efficient DNA repair and chemotherapy resistance, Nature. 631 (2024) 663-669. https://doi.org/10.1038/s41586-024-07620-9.

[29] M. Liu, D. Zhang, X. Zhou, et al., Cell-free fat extract improves ovarian function and fertility in mice with premature ovarian insufficiency, Stem Cell Res Ther. 13 (2022) 320. https://doi.org/10.1186/s13287-022-03012-w.

[30] N. Zhang, Y. Zhang, J. Xu, et al., α-myosin heavy chain lactylation maintains sarcomeric structure and function and alleviates the development of heart failure, Cell Research. 33 (2023) 679-698. https://doi.org/10.1038/s41422-023-00844-w.

[31] Y. Huang, C. Hu, H. Ye, et al., Inflamm-Aging: A New Mechanism Affecting Premature Ovarian Insufficiency, Journal of Immunology Research. 2019 (2019) 1-7. https://doi.org/10.1155/2019/8069898.

[32] J. Petrikova, I. Lazurova, Ovarian failure and polycystic ovary syndrome, Autoimmun Rev. 11 (2012) A471-478. https://doi.org/10.1016/j.autrev.2011.11.010.

[33] W.A.I. Khallaf, E.E. Sharata, M.E. Attya, et al., LCZ696 (sacubitril/valsartan) mitigates cyclophosphamide-induced premature ovarian failure in rats; the role of TLR4/NF-kappaB/NLRP3/Caspase-1 signaling pathway, Life Sci. 326 (2023) 121789. https://doi.org/10.1016/j.lfs.2023.121789.

[34] D. Chen, N. Hu, S. Xing, et al., Placental mesenchymal stem cells ameliorate NLRP3 inflammasome-induced ovarian insufficiency by modulating macrophage M2 polarization, J Ovarian Res. 16 (2023) 58. https://doi.org/10.1186/s13048-023-01136-y.

[35] W. Dong, J. Li, Z. Zhuang, Deciphering the prognostic significance of anoikis-related lncRNAs in invasive breast cancer: from comprehensive bioinformatics analysis to functional experimental validation, Aging (Albany NY). 16 (2024) 402-430. https://doi.org/10.18632/aging.

[36] Y. Yin, H. Li, Y. Qin, et al., Moxibustion mitigates mitochondrial dysfunction and NLRP3 inflammatory activation in cyclophosphamide-induced premature ovarian insufficiency rats, Life Sci. 314 (2023) 121283. https://doi.org/10.1016/j.lfs.2022.121283.

[37] M. Orisaka, K. Tajima, B.K. Tsang, et al., Oocyte-granulosa-theca cell interactions during preantral follicular development, J Ovarian Res. 2 (2009) 9. https://doi.org/10.1186/1757-2215-2-9.

[38] J. Fontana, S. Martinkova, J. Petr, et al., Metabolic cooperation in the ovarian follicle, Physiol Res. 69 (2020) 33-48. https://doi.org/10.33549/physiolres.934233.

[39] J.S. Stroud, D. Mutch, J. Rader, et al., Effects of cancer treatment on ovarian function, Fertil Steril. 92 (2009) 417-427. https://doi.org/10.1016/j.fertnstert.2008.07.1714.

[40] N. Spears, F. Lopes, A. Stefansdottir, et al., Ovarian damage from chemotherapy and current approaches to its protection, Hum Reprod Update. 25 (2019) 673-693. https://doi.org/10.1093/humupd/dmz027.

[41] J. Yoshino, K.F. Mills, M.J. Yoon, et al., Nicotinamide mononucleotide, a key NAD(+) intermediate, treats the pathophysiology of diet- and age-induced diabetes in mice, Cell Metab. 14 (2011) 528-536. https://doi.org/10.1016/j.cmet.2011.08.014.

[42] C.C.S. Chini, T.R. Peclat, G.M. Warner, et al., CD38 ecto-enzyme in immune cells is induced during aging and regulates NAD(+) and NMN levels, Nat Metab. 2 (2020) 1284-1304. https://doi.org/10.1038/s42255-020-00298-z.

[43] K. Okabe, K. Yaku, Y. Uchida, et al., Oral Administration of Nicotinamide Mononucleotide Is Safe and Efficiently Increases Blood Nicotinamide Adenine Dinucleotide Levels in Healthy Subjects, Front Nutr. 9 (2022) 868640. https://doi.org/10.3389/fnut.2022.868640.

[44] S.D. Sullivan, P.M. Sarrel, L.M. Nelson, Hormone replacement therapy in young women with primary ovarian insufficiency and early menopause, Fertil Steril. 106 (2016) 1588-1599. https://doi.org/10.1016/j.fertnstert.2016.09.046.

[45] L.B. Ivashkiv, The hypoxia-lactate axis tempers inflammation, Nat Rev Immunol. 20 (2020) 85-86. https://doi.org/10.1038/s41577-019-0259-8.

[46] W. Liu, Y. Wang, L.H.M. Bozi, et al., Lactate regulates cell cycle by remodelling the anaphase promoting complex, Nature. 616 (2023) 790-797. https://doi.org/10.1038/s41586-023-05939-3.

[47] Z. Ji, G.H. Liu, J. Qu, Mitochondrial sirtuins, metabolism, and aging, J Genet Genomics. 49 (2022) 287-298. https://doi.org/10.1016/j.jgg.2021.11.005.

[48] S. Imai, L. Guarente, NAD+ and sirtuins in aging and disease, Trends Cell Biol. 24 (2014) 464-471. https://doi.org/10.1016/j.tcb.2014.04.002.

[49] J.D. Rabinowitz, S. Enerback, Lactate: the ugly duckling of energy metabolism, Nat Metab. 2 (2020) 566-571. https://doi.org/10.1038/s42255-020-0243-4.

[50] H. Gong, H. Zhong, L. Cheng, et al., Post-translational protein lactylation modification in health and diseases: a double-edged sword, J Transl Med. 22 (2024) 41. https://doi.org/10.1186/s12967-023-04842-9.

[51]Y. Zhang, L. Luo, X. Xu, et al., Acetylation is required for full activation of the NLRP3 inflammasome, Nat Commun. 14 (2023) 8396. https://doi.org/10.1038/s41467-023-44203-0.

[52] D. Zhang, Z. Tang, H. Huang, et al., Metabolic regulation of gene expression by histone lactylation, Nature. 574 (2019) 575-580. https://doi.org/10.1038/s41586-019-1678-1.

[53] L. Wei, X. Yang, J. Wang, et al., H3K18 lactylation of senescent microglia potentiates brain aging and Alzheimer's disease through the NFkappaB signaling pathway, J Neuroinflammation. 20 (2023) 208. https://doi.org/10.1186/s12974-023-02879-7.

[54] J. Wang, Z. Wang, Q. Wang, et al., Ubiquitous protein lactylation in health and diseases, Cell Mol Biol Lett. 29 (2024) 23. https://doi.org/10.1186/s11658-024-00541-5.

[55] S. Hu, Z. Yang, L. Li, et al., Salvianolic Acid B Alleviates Liver Injury by Regulating Lactate-Mediated Histone Lactylation in Macrophages, Molecules. 29 (2024) https://doi.org/10.3390/molecules29010236.

[56] P.T. Morse, T. Arroum, J. Wan, et al., Phosphorylations and Acetylations of Cytochrome c Control Mitochondrial Respiration, Mitochondrial Membrane Potential, Energy, ROS, and Apoptosis, Cells. 13 (2024) https://doi.org/10.3390/cells13060493.

[57] X. Zhang, Y. Wang, H. Li, et al., Insights into the post-translational modifications in heart failure, Ageing Res Rev. 100 (2024) 102467. https://doi.org/10.1016/j.arr.2024.102467.

[58] O. Oktem, B. Urman, Understanding follicle growth in vivo, Hum Reprod. 25 (2010) 2944-2954. https://doi.org/10.1093/humrep/deq275.

[59] R. Li, F. Zhao, H. Diao, et al., Postweaning dietary genistein exposure advances puberty without significantly affecting early pregnancy in C57BL/6J female mice, Reprod Toxicol. 44 (2014) 85-92. https://doi.org/10.1016/j.reprotox.2013.12.003.